Stem Cells and Development

DOI: 10.1089/scd.2018.0181

A *SMN2* splicing modifier rescues the disease phenotypes in an *in vitro* human spinal muscular atrophy model

Ye Seul Son[1,2,†], Kwangman Choi[3,†], Hana Lee[1,2], Ohman Kwon[1], Kwang Bo Jung[1,2], Sunwha Cho[1], Jiyeon Baek[3], Bora Son[3], Sung-Min Kang[1], Mingu Kang[3,4], Jihee Yoon[1,3], Haihong Shen[5], Sangku Lee[3], Jung-Hwa Oh[6], Hyang-Ae Lee[6], Mi-Ok Lee[1], Hyun-Soo Cho[1,2], Cho-Rok Jung[1,2], Janghwan Kim[1,2,*], Sungchan Cho[3,4,*] and Mi-Young Son[1,2,*]

[1]Stem Cell Convergence Research Center, Korea Research Institute of Bioscience and Biotechnology (KRIBB), 125 Gwahangno, Yuseong-gu, Daejeon 34141, Republic of Korea, [2]Department of functional genomics, KRIBB School of Bioscience, Korea University of Science and Technology (UST), 217 Gajeong-ro, Yuseong-gu, Daejeon 34113, Republic of Korea, [3]Natural Medicine Research Center, KRIBB, Cheongju, Chungbuk, Republic of Korea, [4]Department of Biomolecular Science, KRIBB School of Bioscience, UST, 217 Gajeong-ro, Yuseong-gu, Daejeon 34113, Republic of Korea, [5]School of life Sciences, Gwangju Institute of Science and Technology, Gwangju, Republic of Korea, [6]Korea Institute of Toxicology, Daejeon 34114, Republic of Korea

[†]Both authors contributed equally to this work.

[*]Correspondence: Mi-Young Son (E-mail: myson@kribb.re.kr; Tel: 82-42-860-4426; Fax 82-42-860-4608), Sungchan Cho (E-mail: sungchan@kribb.re.kr; Tel: 82-43-240-6105; Fax: 82-43-240-6159), and Janghwan Kim (E-mail: janghwan.kim@kribb.re.kr; Tel: 82-42-860-4478 4479; Fax 82-42-860-4608)

Running title: Efficient SMN rescue in SMA-iPSC model

E mail address: Ye Seul Son (ysson@kribb.re.kr), Kwangman Choi (m84choi@naver.com), Hana Lee (hnlee@kribb.re.kr), Ohman Kwon (omkwon@kribb.re.kr), Kwang Bo Jung (kbjung@kribb.re.kr), Sunwha Cho (swcho@kribb.re.kr), Jiyeon Baek (qor0307@kribb.re.kr), Bora Son (brson@kribb.re.kr), Sung-Min Kang (smkang@kribb.re.kr), Mingu Kang (eytro8606@daum.net), Jihee Yoon (skyjh93@kribb.re.kr), Haihong Shen (haihongshen@gist.ac.kr), Sangku Lee

(sangku@kribb.re.kr), Jung-Hwa Oh (jhoh@kitox.re.kr), Hyang-Ae Lee (vanessa@kitox.re.kr), Mi-Ok Lee (molee@kribb.re.kr), Hyun-Soo Cho (chohs@kribb.re.kr), Cho-Rok Jung (crjung@kribb.re.kr), Janghwan Kim (janghwan.kim@kribb.re.kr), Sungchan Cho (sungchan@kribb.re.kr) and Mi-Young Son (myson@kribb.re.kr)

Stem Cells and Development
A *SMN2* splicing modifier rescues the disease phenotypes in an *in vitro* human spinal muscular atrophy model (DOI: 10.1089/scd.2018.0181)
This paper has been peer-reviewed and accepted for publication, but has yet to undergo copyediting and proof correction. The final published version may differ from this proof.

Abstract

Spinal muscular atrophy (SMA) is caused by the mutation or deletion of the survival motor neuron 1 (*SMN1*) gene. Only approximately 10 % of the products of *SMN2*, a paralogue of *SMN1*, are functional full-length SMN proteins, whereas *SMN2* primarily produces alternatively spliced transcripts lacking exon 7. Reduced SMN protein levels in SMA patients lead to progressive degeneration of spinal motor neurons (MNs). Here, we report an advanced platform based on an *SMN2* splicing-targeting approach for SMA drug screening and validation by using an *SMN2* splicing reporter cell line and an *in vitro* human SMA model *via* induced pluripotent stem cell (iPSC) technology. Through drug screening using a robust cell-based luciferase assay to quantitatively measure *SMN2* splicing, the small-molecule candidate compound rigosertib was identified as an *SMN2* splicing modulator that led to enhanced SMN protein expression. The therapeutic potential of the candidate compound was validated in motor neuron progenitors differentiated from SMA patient-derived iPSCs (SMA iPSC-pMNs) as an *in vitro* human SMA model, which recapitulated the biochemical and molecular phenotypes of SMA, including lower levels of full-length SMN transcripts and protein, enhanced cell death, and reduced neurite length. The candidate compound exerted strong splicing correction activity for SMN2 and potently alleviated the disease-related phenotypes of SMA iPSC-pMNs by modulating various cellular and molecular abnormalities. Our combined screening platform representing a pMN model of human SMA provides an efficient and reliable drug screening system and is a promising resource for drug evaluation and the exploration of drug modes of action.

Keywords: spinal muscular atrophy; motor neuron; induced pluripotent stem cell; disease modelling; drug screening; rigosertib

Stem Cells and Development
A *SMN2* splicing modifier rescues the disease phenotypes in an *in vitro* human spinal muscular atrophy model (DOI: 10.1089/scd.2018.0181)
This paper has been peer-reviewed and accepted for publication, but has yet to undergo copyediting and proof correction. The final published version may differ from this proof.

Introduction

Spinal muscular atrophy (SMA) is an inherited autosomal recessive neuromuscular disease characterized by progressive degeneration of spinal motor neurons (MNs), which leads to subsequent muscle weakness and atrophy [1]. SMA is mainly caused by low levels of the survival motor neuron (SMN) protein, which is ubiquitously expressed and regulates RNA processing [2]. Two SMN genes, *SMN1* and *SMN2*, encode human SMN protein [3]. The *SMN1* gene primarily produces the full-length SMN (SMN-FL) protein and is deleted or mutated in most patients with SMA [4]. The *SMN2* gene is present in most SMA patients, and an inverse correlation between *SMN2* copy number and clinical severity of SMA has been shown [5,6]. Although *SMN2* encodes SMN protein, the majority of *SMN2* gene products are truncated, unstable proteins lacking exon 7 (SMNΔ7) with only low levels of functional SMN-FL protein produced due to inefficient splicing of exon 7 [7].

Although the antisense oligonucleotide nusinersen has recently been approved for use by the FDA [8,9], there is still much progress to be made and other new and promising approaches to explore. Until recently, potential treatment strategies have been developed based on the molecular pathophysiology of SMA, such as pharmacological compounds targeting *SMN2* to increase SMN-FL protein or to facilitate correct splicing of *SMN2* [10], the introduction of *SMN1* using vector-mediated gene delivery [11], and non-SMN targeting approaches to protect MNs [12]. Many studies have shown therapeutic efficacy in patient-derived fibroblast-based assays and model animals, such as yeasts, flies, zebrafish, and mice [13]. However, subsequent clinical trials reported, to date, have failed to demonstrate convincing results based on these approaches [14]. Therefore, a proper *in vitro* human SMA model could be a promising route for the development of effective therapies.

For the last decade, drug testing and development systems using patient-derived induced pluripotent stem cell (iPSC) models have been reported for various neurological diseases such as Parkinson's disease, Alzheimer's disease, amyotrophic lateral sclerosis, Huntington's disease, SMA and other neurodevelopmental diseases [15,16]. Analysis of SMA patient-specific iPSCs (SMA iPSCs) has revealed varying degrees of MN loss,

consistent with a neurodegenerative status particularly in MNs [17-19]. MNs derived from SMA iPSCs show increased apoptosis [20] and delayed neurite outgrowth [21]. At the later stages of differentiation, SMA iPSC-derived MNs exhibit a selective reduction in number and size compared with wild-type (WT) iPSC-derived MNs [19]. Several studies have shown that SMA disease-relevant models based on iPSC technology can be applied to develop new platforms for drug assay and developmental studies. Treatment with valproic acid (VPA) and tobramycin, SMN-inducing compounds, induced partial restoration of SMN protein in SMA iPSCs [19]. Specific inhibitors of apoptotic pathways [20], the thyrotropin releasing hormone (TRH) analogue [22], and antioxidant compounds [21] have been shown to increase SMN protein levels in spinal MNs differentiated from SMA iPSCs and, thus, may have potential efficacy in treating SMA.

Here, we describe a human *in vitro* SMA model based on the generation of patient-specific iPSCs. MN progenitors (pMNs) with an ability to undergo terminal differentiation into mature MNs were generated from SMA iPSCs, characterized as imitating the typical phenotypic features of SMA, and served as a reliable drug-discovery platform. Our drug screening approach for SMA has a clear advantage because we used the combined screening strategy of a luciferase reporter assay for the quantitative assessment of *SMN2* splicing followed by an iPSC-based assay by using pMNs derived from SMA iPSCs (SMA iPSC-pMNs). A library of small-molecule compounds was screened using a SMN2-luciferase reporter cell line to identify potential drug candidates that may restore the inclusion of the *SMN2* exon 7. In addition, we validated and characterized in SMA iPSC-pMNs and showed that one candidate compound rescued the pathological disease phenotypes. Our SMA disease model system provides a platform for efficient drug screening and validation of drug candidates.

Materials and Methods

Cell culture

Primary fibroblasts from SMA type I patients (GM09677, GM00232) were obtained from Coriell Cell Repositories (Camden, NJ, USA). Human WT fibroblasts (CRL-2097 and GM08333) were purchased from the American Type Culture Collection (ATCC, Manassas,

Stem Cells and Development
A *SMN2* splicing modifier rescues the disease phenotypes in an *in vitro* human spinal muscular atrophy model (DOI: 10.1089/scd.2018.0181)
This paper has been peer-reviewed and accepted for publication, but has yet to undergo copyediting and proof correction. The final published version may differ from this proof.

VA, USA) and Coriell Cell Repositories, respectively. They were maintained in minimal essential medium (Gibco, Invitrogen, Carlsbad, CA, USA) containing 10 % fetal bovine serum (FBS, Gibco), 2 mM L-glutamine (Gibco), and 1 % penicillin-streptomycin (P/S, Gibco), as described previously [23]. C33A cells stably expressing SMN1- or SMN2-luciferase splicing reporter (SMN1-Luc and SMN2-Luc stable cell lines) and 293T cells stably expressing FL-fused SMNΔ7 protein (FLuc-SMNΔ7 stable cell line) were maintained in Dulbecco's modified Eagle's medium (DMEM; Gibco) with 10 % FBS, 2 mM L-glutamine and 1 % P/S. Mouse myoblast cell line (C2C12) were purchased from the ATCC and cultured in maintenance medium consisting of DMEM high glucose (Gibco) supplemented with 1% P/S and 10% FBS. C2C12 differentiation was induced by switching to the differentiation medium containing DMEM high glucose (Gibco) with 1% P/S and 2% FBS. The medium changed every other day.

Establishment and maintenance of human iPSCs

Healthy control (CRL2097, IMR90) and SMA patient (GM09677, GM00232) fibroblasts were reprogrammed by electroporation with Episomal iPSC Reprogramming Vectors (Cat. No. A14703, Invitrogen) encoding *OCT4*, *SOX2*, *KLF4*, *L-MYC*, *LIN28* and *shRNA-p53* as described previously [24,25]. Five days after electroporation, the cells were re-seeded at 1×10^5/well onto Matrigel (BD Biosciences, San Diego, CA, USA)-coated 6-well plates with iPSC medium comprising DMEM/F12 medium (Gibco) supplemented with 20 % Knockout Serum Replacement (Gibco), 1 mM non-essential amino acids (Gibco), 0.1 mM β-mercaptoethanol (Sigma-Aldrich, St. Louis, MO, USA) and 10 ng/ml basic fibroblast growth factor (R&D systems, Minneapolis, MN, USA). After 14-20 days, human embryonic stem cell (hESC)-like colonies were isolated and expanded for further experiments. iPSCs were passaged with clump dissociation using 1 mg/ml collagenase type IV (Gibco).

Chemicals

Small-molecule compounds including rigosertib (Selleckchem, Houston, TX, USA), suberoylanilide hydroxamic acid (SAHA) (Selleckchem), cycloheximide (CHX, Sigma-Aldrich), MG132 (Calbiochem, San Diego, CA, USA) sodium butyrate (SB, Sigma-Aldrich), BI2536

(Sigma-Aldrich), GSK461364 (Selleckchem), HMN214 (Selleckchem), and BI6727 (Selleckchem) were used.

Analysis of alternative splicing of SMN pre-mRNA

SMN1-Luc and SMN2-Luc cells were generated by introducing *SMN1* and *SMN2* splicing minigene reporter plasmids, respectively, into C33A cells [26,27]. SMN splicing minigene reporters were designed by the following procedure. Briefly, to inactivate the authentic translation termination codon at the 3' end of exon 7, a single nucleotide 'C' was inserted immediately ahead of the termination codon (CUAA). A FL reporter gene was fused to 21 nucleotides downstream from the 5' end of exon 8, and the initiation codon at the 5' end of the reporter gene was modified by removing the 'A', thereby preventing any undesirable internal translation initiation and reducing background expression. To screen small-molecule compounds that modulate the splicing of *SMN2* pre-mRNA, SMN2-Luc cells were split at a density of 1×10^4 cells/well in 96-well plates. A luciferase assay was performed 24 hours after treatment with small-molecule compounds using a One-Glo Luciferase Assay System (Promega, Madison, WI, USA).

Cell-based SMN immunoassay

SMA patient fibroblasts (8×10^3 cells/well) were seeded on black-well clear bottom 96-well plates (Greiner, Wemmel, Belgium) and treated with small-molecule compounds (10 μM) for 24 hours. MG132, a proteasome inhibitor previously characterized as an SMN-elevating compound [28] was also included as a positive control. Cells were washed and fixed with 4 % paraformaldehyde (PFA). The cells were permeabilized in 0. 5 % Triton X-100 and 1 % bovine serum albumin (BSA) in PBS and incubated with mouse monoclonal antibody against SMN (Cat No. 610647, BD Transduction Laboratories, Franklin Lakes, NJ, USA) for 2 hours. Then, cells were incubated in Alexa Fluor 488-conjugated goat secondary antibody against mouse IgG (Invitrogen) for 1 hour and stained with a Hoechst 33342 dye (Invitrogen). Cell were analysed with a Cellomics ArrayScan instrument (Cellomics, Pittsburgh, PA, USA). More than 300 cells for each sample were analysed to obtain the average and the standard deviation.

Stem Cells and Development
A *SMN2* splicing modifier rescues the disease phenotypes in an *in vitro* human spinal muscular atrophy model (DOI: 10.1089/scd.2018.0181)
This paper has been peer-reviewed and accepted for publication, but has yet to undergo copyediting and proof correction. The final published version may differ from this proof.

Analysis of SMN2 promoter activity

To construct *SMN2* promoter-driven FL reporter plasmids, the promoter and the 5' end of 5'-UTR of the *SMN2* gene (~ 3.4 kb) were cloned into the pGL4.14 vector (Promega). To enhance the responsiveness of the reporter to the change in transcription, a PEST sequence was added to the C-terminus of the FL protein. 293T cells were transfected with 2 μg of pGL4.14-*SMN2* promoter-Luc-PEST reporter plasmid using X-tremeGENE siRNA Transfection Reagent (Roche, Indianapolis, IN, USA) and split at a density of 1×10^4 cells/well in 96-well plates. After 12 hours, cells were treated with rigosertib, SAHA and SB for 24 hours and assayed for luciferase activity by using a One-Glo Luciferase Assay System (Promega). Cell viability was measured in the same conditions by a CellTiter-Glo Luminescent Cell Viability assay (Promega).

Analysis of SMNΔ7 protein stability

To construct plasmids expressing FLuc-SMNΔ7 protein, the FL gene was cloned into the pcDNA3.1 vector, and SMNΔ7 was then inserted into the pcDNA3.1-Fluc vector [29]. 293T cells were transfected with 2 μg of plasmids and treated with 300 μg/ml hygromycin B for 2 weeks for stable selection. Stable cell lines were split at a density of 1×10^4 cells/well in 96-well plates. After 12 hours, cells were treated with various concentrations of rigosertib in the presence of CHX (0.1 mg/mL). Proteasomal inhibitor MG132 (10 μM) was also included as a positive control. A luciferase assay was performed using a One-Glo Luciferase Assay System at 10 hours after treatment. Cell viability was measured in the same conditions by a CellTiter-Glo Luminescent Cell Viability assay.

Total RNA preparation and PCR analysis

Total RNA isolation was performed with an RNeasy Mini Kit (Cat. No. 74104, Qiagen, Hilden, Germany) according to the manufacturer's instructions, and a Superscript IV First-Strand Synthesis System Kit (Cat. No. 18091200, Thermo Fisher Scientific, Waltham, MA, USA) was used for cDNA synthesis. Semi-quantitative RT-PCR was carried out under the following conditions: 3 min at 94 °C; 32-35 cycles of 30 s at 94 °C, 40 s at 55 °C, 40 s at 72 °C, and 5 min extension at 72 °C. Each PCR products were loaded onto 2 % agarose gel

Stem Cells and Development
A *SMN2* splicing modifier rescues the disease phenotypes in an *in vitro* human spinal muscular atrophy model (DOI: 10.1089/scd.2018.0181)
This paper has been peer-reviewed and accepted for publication, but has yet to undergo copyediting and proof correction. The final published version may differ from this proof.

containing SYBR Safe DNA gel stain (Cat No. S33102, Invitrogen) and Gel-Doc (Biorad, Hercules, California, USA) was used for imaging. Quantitative real-time PCR (qRT-PCR) was performed with SYBR green PCR Master mix (Applied Biosystems, Foster City, CA, USA), and the reaction was detected in a 7500 Fast Real-time PCR system (Applied Biosystems) as described previously [30]. Glyceraldehyde-3-phosphate dehydrogenase (GAPDH) was used as an internal standard, and the provided software was used to calculate the CT values of the target genes. The used primers sequences are listed in Supplementary Table S1.

Alkaline phosphatase (AP) and immunocytochemistry

AP staining was performed using naphthol/Fast Red Violet solution (Sigma-Aldrich) as described previously [31,32]. For immunocytochemistry staining, the cells were fixed in 4 % PFA, permeabilized with 0.1 % Triton X-100. After blocking, cells were incubated with the respective primary antibodies at 4 °C overnight, followed by incubation in fluorescence-conjugated secondary antibodies for 2 hr. Slides were observed under an Axiovert 200 M microscope (Carl Zeiss, Gottingen, Germany) or a confocal microscope (Cat. No. FV1000 Live, OLYMPUS, Tokyo, Japan). The used primary antibodies are described in Supplementary Table S2.

Confirmation of karyotype and Short tandem repeat (STR) analysis

Chromosomal G-band karyotyping analysis was performed by GenDix Inc. (Seoul, Republic of Korea). For STR analysis, gDNA preparation of fibroblast and iPSCs was performed with DNeasy Blood & Tissue Kits (Cat. No. 69504, Qiagen) according to the manufacturer's instructions. STR genotyping was analysed by HumanPass Inc. (Seoul, Republic of Korea).

Embryoid bodys (EBs) and teratoma formation assay

For analysis of *in vitro* differentiation capacity, iPSCs were dissociated using 1mg/ml collagenase type IV (gibco) and replated onto non-coated dishes in EB medium supplemented with 10% of knockout serum replacement (gibco) based on DMEM/F12 (gibco). After 5 days, EBs were attached to matrigel-coated LabTek chamber slides (Nunc, Rochester NY, USA) and cultured for 10 days. iPSCs (1×10^6 cells) were subcutaneously

Stem Cells and Development
A *SMN2* splicing modifier rescues the disease phenotypes in an *in vitro* human spinal muscular atrophy model (DOI: 10.1089/scd.2018.0181)
This paper has been peer-reviewed and accepted for publication, but has yet to undergo copyediting and proof correction. The final published version may differ from this proof.

injected into 6-week-old BALB/c-nude mice (Orient Bio Inc, Seoul, Korea). The resulting teratomas were fixed by 10 % formaldehyde, paraffin-embedded, serially sectioned, and stained using haematoxylin & eosin staining (H&E) solution (Sigma-Aldrich). Teratoma assays were performed after approval by the Institutional Animal Care and Use Committee (IACUC) of KRIBB (approval No: KRIBB-AEC-17014).

Differentiation toward MNs

MNs were differentiated as described previously [33]. Neural induction media contained DMEM/F12 medium and neurobasal media at a 1:1 ratio supplemented with 1 % P/S, 1 % GlutaMAX (Gibco), 100 nM L-ascorbic acid (Santacruz Biotechnology, Delaware, CA, USA), 0.5× N-2 supplements (Gibco), and 0.5x B-27 supplement (Gibco). iPSCs were dissociated using 1 mg/ml collagenase type IV and 1 mg/ml dispase (Invitrogen). Detached iPSCs were cultured on non-coated petri dishes with NEP media containing 3 μM CHIR99021 (Torcris, Ballwin, MO, USA), 2 μM DMH-1 (Stemgent, Texas, Houston, USA), and 2 μM SB431542 (Stemgent), and the culture medium was changed every other day. After 6 days, NEPs were dissociated with 1 mg/ml dispase and differentiated into pMNs with neural induction media supplemented with 1 μM CHIR99021, 2 μM DMH-1, 2 μM SB431542, 0.1 μM retinoic acid (RA, Stemgent), and 0.5 μM purmorphamine (Pur, Stemgent). The pMN induction medium was changed every other day. The pMNs were sub-cultured once a week, using McIlwainTM tissue chopper (Mickle Engineering, Gomshall, UK) and cultured in pMN induction medium supplemented with 0.5 mM VPA (Stemgent); the medium was changed every other day. The pMNs were frozen with Recovery™ Cell Culture Freezing Medium (Gibco) and stored in liquid nitrogen. For further differentiation into MNs, $HB9^+$ MNs were generated by culturing dissociated pMNs in MN induction medium supplemented with 0.5 μM RA and 0.1 μM Pur, and the medium was changed every other day. After 6 days, induction of $ChAT^+$ and $SMI32^+$ MNs were dissociated into single cells using Accumax (eBioscience, San Diego, CA, USA), seeded on Matrigel coated-dishes, and cultured with MNs medium supplemented with 0.1 mM compound E (Calbiochem, Darmstadt, Germany) for 10 days. All differentiation experiments were independently performed at least three times.

Western blot analysis

The pMNs and MNs were harvested at indicated times. The cells were lysed with RIPA buffer containing 1 mM protease inhibitor and 1×PMSF. The, 20 μg of the cell lysate was resolved by precast gels (4-15 % gradient, Bio-Rad Laboratories, Hercules, CA, USA). After transfer, the membranes were incubated with the appropriate primary antibody, washed, and incubated with the secondary antibody. The list of primary antibodies used is given in Supplementary Table S2. The band intensity was quantified using ImageJ software (National Institutes ofHealth, Bethesda,MD, USA).

Cell viability and death analysis

To detect LIVE/DEAD cells using a LIVE/DEAD Viability/Cytotoxicity Kit (Cat No. L3224, Invitrogen), cells were washed and incubated at room temperature with LIVE/DEAD assay reagent containing 2 μM Calcein-AM and 4 μM EthD-1. After 40 min, cells were washed and visualized with a microscope (IX51, Olympus, Japan). The fluorescence was measured at 494/517 nm and 528/617 nm with Calcein-AM and EthD-1, respectively. To quantify LIVE/DEAD cells, the cells were trypsinized, and 1-2×10^6 cells were stained with LIVE/DEAD assay reagent mixed with 50 μM Calcein-AM and 4 μM EthD-1. The cells were incubated for 20 min at room temperature protected from light and evaluated by flow cytometry (BD Accuri C6; Becton-Dickinson, Mansfield, MA, USA).

Detection of mitochondria and mitochondrial superoxide levels

To monitor mitochondrial contents and mitochondrial superoxide generation, the cells stained with MitoTracker (Cat No. M7514, Invitrogen) and MitoSOX (Cat No. M36008, Invitrogen), respectively. The cells were incubated at 37 °C for 15 min using 250 nM MitoTracker and 5 μM MitoSOX staining solution, protected from light. After staining, the cells were captured at 490/516 nm and 510/580 nm, respectively.

Analysis of neurite outgrowth

MNs cultures on Matrigel coated-dishes were fixed in 4 % PFA. The neurites were stained with TUJ1 according to the immunocytochemistry method. Images were captured on a fluorescence microscope (IX51, Olympus, Japan). Neurite outgrowth was analysed by

NeuronJ (ImageJ add-on software). Each neurite could be observed even if it was curved by using NeuronJ, and 45 neurites per condition were measured and quantified for length [34].

Animal experiments

All animal experiments were performed in accordance with Korean Food and Drug Administration guidelines. All protocols were reviewed and approved by the Institutional Animal Care and Use Committee of KRIBB (institutional permit number: KRIBB-AEC-18132). A heterozygous SMA mouse (FVB.Cg-Grm7$^{Tg(SMN2)89Ahmb}$ Smn1^{tm1Msd} Tg(SMN2*delta7)4299Ahmb/J, stock number 005025) stock number 005025) was purchased from Jackson Laboratory (Bar Harbor, ME, USA) and mated to obtain homozygous SMA mice (SMNΔ7 transgenic mouse). Rigosertib (10 mg/kg) was intraperitoneally administered to SMNΔ7 transgenic mice once a day from postnatal day 3 to 10 (n=3 for each group). On the last day of administration, the spinal cord was isolated from each mouse 5 hours after injection and lysates were prepared by sonicating in RIPA buffer (LPS solution, Daejeon, Korea), containing protease inhibitor cocktail set Ⅲ (Calbiochem). Quantitative western blot analysis was performed as described previously [35]. Quantification of SMN expressed cell population in the spinal cord tissue was performed as described previously [36]. For histological analysis, mouse spinal cords were collected, fixed with 4 % PFA solution and transferred into 30 % sucrose for cryopreservation. The tissues were frozen in optimal cutting temperature compound (Tissue-Tek OCT Compound, Sakura Finetek USA, Inc, Torrance, CA, USA) and sectioned to produce 10 µm-thick sections. All sections were permeabilized in 0.01 % Triton X-100 for 15 min and incubated overnight with primary antibodies at 4 ℃. After washing 3 times, sections were incubated with secondary antibody at room temperature for 1 hr. The tissues were captured by using the Evos Fl Auto 2 Cell Imaging System (Thermo Fisher Scientific). The primary antibodies used are described in Supplementary Table S2.

Neuromuscular junction (NMJ) formation assay

To identify functionality of hiPSC-derived motor neurons, the C2C12 cells were plated onto Matrigel-coated confocal dish at a density of 880 cells/mm^2 in maintenance medium. After

Stem Cells and Development
A *SMN2* splicing modifier rescues the disease phenotypes in an *in vitro* human spinal muscular atrophy model (DOI: 10.1089/scd.2018.0181)
This paper has been peer-reviewed and accepted for publication, but has yet to undergo copyediting and proof correction. The final published version may differ from this proof.

24 hr, myoblast fusion was induced by transferring the cells to the differentiation medium. The media were changed every other day. On day 4, HB9+ MN were dissociated and seeded onto myotubes at a density of 8800 cells/mm^2. The cells were cultured with ChAT+ MN, in a differentiation medium, containing neurotrophic factors (10 ng/ml Insulin-like growth factor 1 (Peptrotech, Rocky Hill, NJ, USA), 10 ng/ml Brain-derived neurotrophic factor (BDNF, Peptrotech), and 10 ng/ml ciliary neurotrophic factor (CNTF, R&D systems) for 7 days. For evaluation of the NMJ, overlapping region quantification of α-Bungarotoxin-488 and ChAT+ were performed. NMJ measurements were performed every sixth fields the co-culture condition of iPSC-derived MNs and C2C12 cells.

Electrophysiological recordings

Whole-cell patch-clamp recordings were carried out to measure action potential (AP) and voltage-gated sodium/potassium currents. Terminally differentiated MNs plated on coverslips were placed in a recording chamber and continuously perfused (3 mL/min) with bath solution contained (in mM): 137 NaCl, 2.0 $CaCl_2$, 10 HEPES, 20 glucose (pH 7.3 with NaOH). The patch pipettes were made from borosilicate glass capillaries (Clark Electromedical Instruments, UK) using a pipette puller (PP-830, Narishige, Japan). Their resistances were 5-8 MΩ when filled with pipette solution contained (in mM): 140 K-gluconate, 5 NaCl, 1 $MgCl_2$, 0.5 EGTA, 10 HEPES (pH 7.25 with KOH). Voltage- or Current-clamp protocol generation and data acquisition were controlled by computers equipped with an A/D converter, Digidata 1440 (Molecular Devices, Sunnyvale, CA USA) and pClamp 10.3 software (Molecular Devices). The signals were filtered at 5 kHz and sampled at 10 kHz using Axopatch 200B amplifier (Molecular Devices). Evoked APs were induced by injections of step currents from -0.1 to 0.2 nA in 0.02 nA increments for 500 ms. For the voltage-gated currents, we used voltage steps for 1 s from −70 to +90 mV in 10 mV increments. Clamfit (Molecular Devices), GraphPad Prism version 5 (GraphPad Software Inc., San Diego, CA, USA), and Origin (Microsoft, Redmond, Washington, USA) were used for data analysis.

Statistics

The statistical significance of the difference between two independent samples was analysed using the non-parametric Mann-Whitney U-test. Experimental Results were

expressed as mean value ± standard error of the mean (SEM), and statistically significant differences were indicated on the graph by asterisks (ns: not significant, *P<0.05, **P<0.01, ***P<0.001). All experiments were repeated at least three times.

Results

Screening for SMN2 splicing modulators

As a splicing defect in *SMN2* is a major factor that causes the disease phenotype in SMA patients, the recovery of *SMN2* splicing is a promising therapeutic approach for the treatment of SMA [37]. Therefore, we developed a new platform for SMA drug development that combines a luciferase reporter assay for the quantitative assessment of *SMN2* splicing followed by validation of drug candidates using a patient-specific iPSC-based assay (Fig. 1A). For a facile and quantitative measurement of *SMN2* splicing, we developed a robust cell-based assay system (SMN2-luciferase splicing reporter cell line; SMN2-Luc stable cell line), which harbours an exogenously introduced *SMN2* minigene consisting of exons 6 through 8 and intervening introns, fused with the firefly luciferase (FLuc) gene (Fig. 1B). In this assay system, any compound that enhances the inclusion of exon 7 would increase FLuc activity because exon 7-included mRNAs would produce a larger protein fused with FLuc protein. In contrast, exon 7-skipped mRNAs generate an in-frame translational termination codon at exon 8, resulting in the production of pre-maturely terminated proteins without the fusion of FLuc protein. After treatment with 88 small-molecule compounds, we identified 2 compounds (No. 53 and No. 65) that notably increased the luciferase activity by more than 3-fold of the DMSO control (Fig. 1C). The SMN1-Luc stable cell line, harbouring the *SMN1* minigene reporter, was additionally tested as a control to evaluate the specificity of the effect on *SMN2* splicing, and no enhancement of luciferase activity was found (Supplementary Fig. S1).

The candidate compound rigosertib promotes splicing correction of SMN2 exon 7

Next, we examined whether these two compounds increased the amount of SMN protein in SMA fibroblasts from an SMA type I patient. We performed an immunoassay to specifically detect SMN protein by using its specific antibody, which provided a quantitative measurement of SMN protein inside the cells. Of the two compounds, only

Stem Cells and Development
A *SMN2* splicing modifier rescues the disease phenotypes in an *in vitro* human spinal muscular atrophy model (DOI: 10.1089/scd.2018.0181)
This paper has been peer-reviewed and accepted for publication, but has yet to undergo copyediting and proof correction. The final published version may differ from this proof.

compound No. 65 induced a significant increase in SMN protein (1.62-fold of the DMSO control) (Fig. 2A). Thus, subsequent studies were conducted only with compound No. 65, which was rigosertib (ON 01910.Na), a well-known PLK (Polo-like kinase) inhibitor [38]. To further define whether the effect of rigosertib on *SMN2* splicing is related to PLK inhibition, four other PLK inhibitors (BI2536, GSK461364, HMN214 and BI6727) were also tested in SMN2-Luc cells. Of the five tested PLK inhibitors, rigosertib exhibited the strongest effect, increasing the luciferase activity in SMN2-Luc cells by approximately 4-fold at 100 and 1,000 nM, while the other inhibitors had little or no effect on luciferase activity (Fig. 2B). Rigosertib had a marginal effect on the luciferase activity in SMN1-Luc cells (Fig. 2B). Collectively, these results indicate that rigosertib exerts strong splicing correction activity on *SMN2* and that the activity is not related with PLK inhibition.

We further investigated whether rigosertib could increase the expression of SMN protein by other mechanisms. To analyse the effect of rigosertib on *SMN2* transcriptional activation, we constructed a luciferase reporter vector containing the *SMN2* promoter by fusing with a PEST sequence to reduce the protein half-life of firefly luciferase. We found that there was no significant change in transcriptional activity with rigosertib (Fig. 2C), whereas the positive control histone deacetylase (HDAC) inhibitors, including SAHA and SB, induced marked effects without affecting cell viability (Supplementary Fig. S2A). A possible effect of rigosertib on SMN protein stability was also examined. Considering that degradation of SMNΔ7 is much more susceptible to the proteasome inhibition [29], we generated 293T cells stably expressing FLuc-fused SMNΔ7 protein (FLuc-SMNΔ7 stable cell lines). Luciferase activity was dramatically decreased by treatment with the protein synthesis inhibitor cycloheximide (CHX) alone, indicating the instability of SMNΔ7. Treatment with MG132 markedly increased the luciferase activity as a result of proteasome inhibition. In contrast, rigosertib had little effect on the degradation of SMNΔ7 (Fig. 2D) with no significant effect on cell viability (Supplementary Fig. S2B). These results clearly excluded the possible involvement of transcription and protein stability in the effect of rigosertib on SMN expression.

Stem Cells and Development
A *SMN2* splicing modifier rescues the disease phenotypes in an *in vitro* human spinal muscular atrophy model (DOI: 10.1089/scd.2018.0181)
This paper has been peer-reviewed and accepted for publication, but has yet to undergo copyediting and proof correction. The final published version may differ from this proof.

Generation of iPSCs from a type 1 SMA patient

To establish a physiologically representative *in vitro* human SMA model, we generated SMA iPSCs from type 1 SMA patient fibroblasts and differentiated SMA iPSCs into disease-relevant cell types for experimental validation of rigosertib. We reprogrammed SMA fibroblasts into iPSCs by using non-integrating oriP/*EBNA-1*-based episomal vectors (Fig. S3A). The properties of SMA iPSCs were confirmed based on their hESC-like morphology and the expression of pluripotency markers, including AP, OCT4, NANOG, TRA-1-60, TRA-1-81, SSEA-3, and SSEA-4 (Fig. S3B and S3C). *In vitro* and *in vivo* differentiation potential of the SMA iPSCs was confirmed by the presence of all three germ layers in EBs (Fig. S3D) and teratomas (Fig. S3E) derived from SMA iPSCs, respectively. Short tandem repeat (STR) analysis verified that SMA iPSCs were derived from the SMA patient's fibroblasts (Fig. S3F) and cultured SMA iPSCs maintained a normal karyotype (Fig. S3G). These results indicated the successful reprogramming of SMA fibroblasts into SMA iPSCs.

Development of in vitro SMA model using SMA iPSC-derived pMN (SMA iPSC-pMN)

SMA is caused by low levels of SMN protein due to the loss of the *SMN1* gene and inefficient splicing of the *SMN2* gene, which primarily affects α-MNs of the lower spinal cord [39]. Therefore, to observe disease-relevant phenotypes, we differentiated WT iPSCs and SMA iPSCs into MNs *via* highly pure pMN (Fig. 3A and Supplementary Fig. S4A) using a previously described method with some modifications [33]. Control iPSCs derived from WT human fibroblasts and SMA iPSCs were differentiated into neuroepithelial progenitors (NEPs) in the presence of SB431542 (inhibitor of activin-nodal signalling), DMH1 (inhibitor of bone morphogenetic protein signalling), and CHIR99021 (Wnt agonist), which were then treated with RA for caudalization and with Pur (SHH signalling agonist) for ventralization [40]. A robust population of OLIG2+ pMNs were isolated and suspended at 12 days after differentiation from iPSCs with almost no interneuron progenitors, labelled by NKX2.2. For terminal differentiation, OLIG2+ pMNs were treated with RA and Pur suspension to induce differentiation into HB9+ and ISL1+ pre-mature MNs, which then were further differentiated into mature ChAT+ and SMI32+ MNs in the presence of Compound E for 10 days (Fig. 3B and Supplementary Fig. S4B). Furthermore, the percentage of OLIG2+ and

Stem Cells and Development
A *SMN2* splicing modifier rescues the disease phenotypes in an *in vitro* human spinal muscular atrophy model (DOI: 10.1089/scd.2018.0181)
This paper has been peer-reviewed and accepted for publication, but has yet to undergo copyediting and proof correction. The final published version may differ from this proof.

ChAT+ cells in the differentiated pMNs and MNs remained similar in WT and SMA groups with over 75.6 % of OLIG2+ and 85.5 %of ChAT+, respectively (Fig. 3C). These data imply that there was no significant difference in differentiation potential between WT and SMA groups. Importantly, most of the pMNs derived from WT iPSCs and SMA iPSCs were highly proliferative, as shown by Ki67 expression, and the pMNs were expanded for at least five passages, along with robust OLIG2 expression (Fig. 3D and Supplementary Fig. S4C). Furthermore, OLIG2+ pMNs can be frozen, thawed and then terminally differentiated into mature ChAT+ MNs when needed.

During pMN and MN differentiation, the cells differentiated from SMA iPSCs exhibited different and even defective characteristics compared with WT cells. First, RT-PCR analysis revealed that SMA iPSC-pMNs and SMA iPSC-MNs had lower levels of SMN-FL transcripts, including *SMN1* and *SMN2*, with SMN-FL band intensities of 21.54 % in SMA#1-pMNs and 26.55 % in SMA#2-pMNs compared with WT iPSC-pMNs and 33.98 % in SMA#1-MNs, 25.44 % in SMA#2-MNs, compared with WT iPSC-MNs, respectively, and higher levels of SMNΔ7 transcripts (Fig. 4A). Second, at the protein level, the expression of SMN-FL protein in SMA iPSC-pMNs and SMA iPSC-MNs was significantly decreased, with reductions of 16.82 % in SMA#1-pMNs and 35.19 % in SMA#2-pMNs, when compared with that in WT pMN controls and 27.73 % in SMA#1-MNs and 30.27 % in SMA#2-MNs, when compared with that in WT MN controls, respectively, as shown in western blot (Fig. 4B) and immunocytochemistry (Fig. 4C) analyses. Nuclear gem bodies were rarely present in SMA iPSC-pMNs and SMA iPSC-MNs (Fig. 4C). These results showed a reduced level of functional SMN-FL protein in SMA iPSC-pMNs and SMA iPSC-MNs. Third, as reported here and previously by another group [20,41], enhanced cell death was observed in the SMA cells (1.59-fold in SMA#1-pMNs, 1.77-fold in SMA#2-pMNs and 1.71-fold in SMA#1-MNs, 1.76-fold in SMA#2-MNs, respectively) compared with WT cells (Fig. 4D). Fourth, the neurite length in SMA iPSC-MNs was much shorter (approximately 70.92 % in SMA#1-MNs and 79.77% in SMA#2-MNs, respectively) than that of WT#1 iPSC-MNs (Fig. 4E), consistent with previous studies [17,42]. Furthermore, when terminally differentiated WT and SMA iPSC-MNs were co-cultured with differentiated myotubes from mouse C2C12 cells for the formation of NMJ, we observed that aggregated α-bungarotoxin (α-BTX) acetylcholine

Stem Cells and Development
A *SMN2* splicing modifier rescues the disease phenotypes in an *in vitro* human spinal muscular atrophy model (DOI: 10.1089/scd.2018.0181)
This paper has been peer-reviewed and accepted for publication, but has yet to undergo copyediting and proof correction. The final published version may differ from this proof.

receptors (AChR) on myotubes were overlapping with ChAT neurites in WT iPSC-derived MNs, suggesting the formation of NMJ. However, AChR clustering on myotubes co-cultured with SMA iPSC-derived MNs were remarkably impaired (Supplementary Fig. S5). Additionally, we evaluated whether the terminally differentiated MNs from WT and SMA iPSCs have functional membrane properties using electrophysiological analysis. When currents (from -0.1 nA to 0.2 nA with 0.02 nA steps for 500 ms) were injected into MNs, an AP was fired (Vm > 0 mV) on WT iPSC-derived MNs up to 0.2 nA, however, the multiple APs were induced on SMA iPSC-derived MNs (Supplementary Fig. S6A and B). The average Na^+ current (I_{Na}) in control MNs were −54.8 ± 6.4 pA/pF for WT#1 iPSC-MNs and−53.7 ± 8.3 pA/pF for WT#2 iPSC-MNs, compared with −74.3 ± 14.7 pA/pF in SMA#1 iPSC-MNs and −85.2 ± 10.8 pA/pF in SMA#2 iPSC-MNs (Supplementary Fig. S6C-E). Thus, our data demonstrate that SMA MNs are more readily excitable than WT MNs with higher AP firing and I_{Na} current density in accordance with previous reports [43]. Taken together, these data imply that both SMA iPSC-pMNs and SMA iPSC-MNs in our culture system were useful for analysing SMA pathology and could be applied to an *in vitro* disease model. SMA iPSC-pMNs were selected for further experiments due to their advantages, such as the more significant reduction in SMN-FL transcripts and proteins and their ability to quickly yield a sufficient quantity for performing cell culture-based assays.

Cellular damage in SMA iPSC-pMNs caused by the splicing defect of SMN2 can be rescued by rigosertib treatment

The selected candidate rigosertib from the primary screening using the SMN2-Luc stable cell lines was demonstrated to exert significant splicing correction activity for *SMN2*. Therefore, we proceeded to test whether rigosertib could alleviate the defective phenotypes by inhibiting splicing of the *SMN2* exon 7 in SMA iPSC-pMNs capable of mimicking the disease phenotypes *in vitro*. Rigosertib increased SMN-FL mRNA levels in SMA iPSC-pMNs after 72 hours of treatment (Fig. 5A). qRT-PCR analysis using the forward primer spanning exon 7 and 8 and the reverse primer for exon 8 [44] revealed that SMA#1 iPSC-pMNs and SMA#2 iPSC-pMNs had lower levels of SMN-FL transcripts with 74.21 % and 50.42 % reductions, respectively, compared with WT#1 iPSC-pMNs (Fig. 5B). There is no significant difference between WT controls. Rigosertib increased mRNA expression of

Stem Cells and Development
A *SMN2* splicing modifier rescues the disease phenotypes in an *in vitro* human spinal muscular atrophy model (DOI: 10.1089/scd.2018.0181)
This paper has been peer-reviewed and accepted for publication, but has yet to undergo copyediting and proof correction. The final published version may differ from this proof.

SMN-FL, by the inclusion of exon 7 in SMA#1 iPSC-pMNs and SMA#2 iPSC-pMNs, by 2.78- and 1.46-fold, respectively. Rigosertib treatment increased the amount of SMN protein in the patient-derived pMNs, as determined by western blot analysis (Fig. 5C) and immunocytochemistry (Fig. 5D), and restored gem body formation in SMA iPSC-pMNs (Fig. 5D). To dissect the protective role of rigosertib in SMA, we examined the effect of rigosertib on the cell death of MNs derived from SMA iPSCs. Application of rigosertib significantly decreased the percentage of dead cells in SMA iPSC-pMNs from 12.86 % and 7.24 % in SMA#1- and SMA#2-pMNs, respectively, to 9.21 % and 3.82 % in rigosertib-treated SMA#1- and SMA#2-pMNs, respectively (p<0.05) (Fig. 5E). Therefore, to understand the mechanisms underlying the cell death caused by reduced levels of SMNs, we compared mitochondrial superoxide production, which is known to be implicated in the functional defects of spinal MNs, in SMA iPSC-pMNs using MitoSOX Red, a mitochondrial superoxide indicator. Significantly more MitoSOX+ cells were observed in SMA iPSC-pMNs than in WT iPSC-pMNs (1.40- and 1.21-fold, p<0.010.05) (Fig. 5F). Rigosertib treatment in SMA iPSC-pMNs decreased the generation of MitoSOX+ cells to a similar level to the WT control (p<0.010.05) (Fig. 5F). Moreover, rigosertib treatment protected against SMN deficiency-induced reduction of neurite outgrowth in terminally differentiated SMA iPSC-MNs, showing a phenotype closer to differentiated WT iPSC-MNs (Fig. 5G). These data suggest that the *SMN2* splicing modifier rigosertib can modulate *SMN2* splicing in favour of exon 7 inclusion and thereby increase the production of SMN protein in an *in vitro human SMA model* and further ameliorate the cell death induced by mitochondrial oxidative stress, which is involved in the degeneration of MNs [21].

Intraperitoneal injection of rigosertib increases SMN protein levels in the spinal cord of SMA mice

To examine whether rigosertib increases the amount of SMN protein *in vivo*, SMNΔ7 transgenic mice at postnatal day 3 were intraperitoneally administered with 10 mg/kg of rigosertib over the course of 8 days. The SMNΔ7 transgenic mouse is the most prevalently used SMA mouse model that presents a severe type of SMA and survives for only two weeks [45]. Five hours after the final rigosertib dosing, the spinal cord extract was prepared and subjected to quantitative western blot analysis with the SMN antibody. The

amount of SMN protein in the spinal cord of rigosertib-treated SMA mice was found to be increased by 2.13-fold compared with that of SMA mice (Fig. 6A and 6B). In addition, we evaluated spinal cord tissue sections from the same mice, histologically. High SMN expression was observed in spinal cord tissue from heterozygous mice, whereas, the SMN protein was very weakly expressed in spinal cords from the SMA mice (Fig. 6C). Consistent with western blotting analysis, SMN+ cell population in the spinal cord was significantly increased in rigosertib-treated mice compared to the SMA mice by 3.18-fold (Fig. 6C and 6D), indicating the effectiveness of rigosertib *in vivo*.

Discussion

Despite the development of promising therapeutic strategies, SMA remains a non-curative neuromuscular disease with no available FDA-approved drug treatment. Though SMA is caused by lack of the *SMN1* gene, *SMN2* is the primary disease-modifying gene in humans [46]. However, these two SMN genes, *SMN1* and *SMN2*, encode SMN protein in humans, whereas most animals have only the *SMN1* gene [3]. This difference makes it difficult to develop proper *in vivo* models capable of faithfully recapitulating human SMA disease. Additionally, MNs are the primarily affected cell type in SMA but are fundamentally difficult to obtain. Patient-specific iPSCs obtained *via* reprogramming technology provide a unique opportunity to model human diseases *in vitro* by directing iPSCs into disease-relevant cell types. Therefore, MNs differentiated from SMA iPSCs represent a useful *in vitro* SMA model for elucidating the molecular and pathological processes associated with SMA and for screening novel therapeutic drug candidates [47].

As SMA is fundamentally caused by reduced SMN protein levels, the recovery of *SMN2* splicing is one of the most promising therapeutic approaches for treating SMA. Accordingly, the administration of small molecules [44,48,49] and antisense oligonucleotides [50,51] that promote the inclusion of exon 7 into *SMN2* mRNA have been reported to correct the SMA phenotypes in mouse models. Two to six copies of the *SMN2* gene have been observed in patient somatic cells [52], and SMN protein levels in patients are generally correlated with *SMN2* gene copy number [53]. In this study, two SMA patient-specific iPSC lines were generated from two SMA type 1 patient's fibroblasts with

Stem Cells and Development
A *SMN2* splicing modifier rescues the disease phenotypes in an *in vitro* human spinal muscular atrophy model (DOI: 10.1089/scd.2018.0181)
This paper has been peer-reviewed and accepted for publication, but has yet to undergo copyediting and proof correction. The final published version may differ from this proof.

homozygous deletion of exons 7 and 8 of the *SMN1* and two or three *SMN2* copies. This genotype did not affect the differentiation of spinal MNs, consistent with a previous report [43]. SMA iPSC-pMNs were generated and characterized as a human SMA model and were used as a testing platform for the validation of the candidate drug, a *SMN2* splicing modifier. We observed relevant SMA phenotypes due to decreased amounts of SMN-FL transcript in SMA iPSC-pMNs, such as increased cell death and reduced neurite length, impaired formation of NMJ and hyperexcitability in SMA iPSC-MNs, in line with previously observed phenotypes [17,18,20,41,42,54]. Moreover, using our model system, we identified augmented mitochondrial ROS production in SMA iPSC-pMNs, leading to MN death, as observed in SMA.

Here, we report the discovery of a novel small molecule that specifically restored *SMN2* splicing in a robust high-throughput cell-based assay system using SMN2-Luc stable cell lines. Out of the 88 tested small molecules, rigosertib was the most efficient compound, selectively modulating *SMN2* splicing to include exon 7 and subsequently increasing SMN protein levels. Rigosertib inhibits the activity of multiple kinases, such as PLK1, by affecting multiple signalling cascades leading to cancer cell death [55,56]. Orally bioavailable rigosertib [57] has recently entered clinical trials against solid tumours and haematological malignancies such as myelodysplastic syndrome (MDS) and has demonstrated promising results [58-60]. However, our results demonstrate that its activity in *SMN2* splicing modulation is not a result of PLK inhibition, the transcription of *SMN2* or the stability of SMN protein. Future identification and characterization of rigosertib as an *SMN2* splicing modifier will help to clarify the molecular basis of its specificity.

Increased SMN levels by rigosertib treatment ameliorated phenotypes of associated with loss of the *SMN1* gene in a human *in vitro* SMA disease model. The rescue of MN death by the reduction of mitochondrial oxidative stress in SMA patient-specific pMNs treated with rigosertib suggested the possible use of this small molecule for SMA treatment. Recent studies have described dysfunction of mitochondria in mouse MNs with knocked down SMN expression using small interfering RNA, implying that SMN is required for normal mitochondrial function [61]. In addition, patients with SMA were reported to have less mitochondrial DNA [62,63] and markedly increased levels of oxidative stress [64].

Stem Cells and Development
A *SMN2* splicing modifier rescues the disease phenotypes in an *in vitro* human spinal muscular atrophy model (DOI: 10.1089/scd.2018.0181)
This paper has been peer-reviewed and accepted for publication, but has yet to undergo copyediting and proof correction. The final published version may differ from this proof.

The application of an antioxidant, such as N-acetylcysteine, has many beneficial effects on MNs, such as reducing mitochondrial oxidative stress in hESC-based SMA model [21]. These observations raise the possibility that mitochondrial dysfunction in SMA models may be a direct consequence of the disruption of SMN functions. Indeed, rigosertib corrected the alternative splicing defects of *SMN2* exon 7 and significantly reduced mitochondrial oxidative stress. To the best of our knowledge, this is the first study reporting the effects of rigosertib treatment as an *SMN2* splicing modifier in an *in vitro* human SMA model. Furthermore, the administration of rigosertib to a SMNΔ7 SMA mouse model led to an increase in SMN protein levels in the spinal cord. However, further experiments are needed to address the relationship between the pathogenesis of SMA by the loss of MNs and abnormal mitochondrial function in SMA and to elucidate the functions of rigosertib in recovering disease-associated phenotypes.

In summary, we established an advanced drug screening and validation platform based on an *SMN2* splicing-targeting approach by using the SMN2-Luc stable cell line and an *in vitro* human SMA model (SMA iPSC-pMNs) and showed that rigosertib can restore SMN protein levels by promoting *SMN2* exon 7 inclusion. Our data provide evidence that SMA iPSC-pMNs recapitulate the disease-specific phenotypes, such as increased cell death and mitochondrial ROS production and that such phenotypes can be reversed by rigosertib. Our findings may contribute to the development of effective therapies for SMA and other neuromuscular disease.

Acknowledgement

This research was supported by the National Research Foundation of Korea (NRF) grant funded by the Korean government (MSIT) (2015M3A9C7030128, NRF-2018M3A9H3023077, NRF-2016K1A1A8A01938649) and a grant from KRIBB Research Initiative Program. The funders had no role in the study design, data collection or analysis, decision to publish, or preparation of the manuscript.

Author Disclosure Statement

No competing financial interests exist.

References

1. Crawford TO and CA Pardo. (1996). The neurobiology of childhood spinal muscular atrophy. Neurobiol Dis 3:97-110.
2. Lefebvre S, L Burglen, J Frezal, A Munnich and J Melki. (1998). The role of the SMN gene in proximal spinal muscular atrophy. Hum Mol Genet 7:1531-6.
3. Coovert DD, TT Le, PE McAndrew, J Strasswimmer, TO Crawford, JR Mendell, SE Coulson, EJ Androphy, TW Prior, et al. (1997). The survival motor neuron protein in spinal muscular atrophy. Hum Mol Genet 6:1205-14.
4. Hahnen E, R Forkert, C Marke, S Rudnik-Schoneborn, J Schonling, K Zerres and B Wirth. (1995). Molecular analysis of candidate genes on chromosome 5q13 in autosomal recessive spinal muscular atrophy: evidence of homozygous deletions of the SMN gene in unaffected individuals. Hum Mol Genet 4:1927-33.
5. Lefebvre S, L Burglen, S Reboullet, O Clermont, P Burlet, L Viollet, B Benichou, C Cruaud, P Millasseau, et al. (1995). Identification and characterization of a spinal muscular atrophy-determining gene. Cell 80:155-65.
6. Rudnik-Schoneborn S, C Berg, K Zerres, C Betzler, T Grimm, T Eggermann, K Eggermann, R Wirth, B Wirth, et al. (2009). Genotype-phenotype studies in infantile spinal muscular atrophy (SMA) type I in Germany: implications for clinical trials and genetic counselling. Clin Genet 76:168-78.
7. Burnett BG, E Munoz, A Tandon, DY Kwon, CJ Sumner and KH Fischbeck. (2009). Regulation of SMN protein stability. Mol Cell Biol 29:1107-15.
8. Finkel RS, CA Chiriboga, J Vajsar, JW Day, J Montes, DC De Vivo, M Yamashita, F Rigo, G Hung, et al. (2016). Treatment of infantile-onset spinal muscular atrophy with nusinersen: a phase 2, open-label, dose-escalation study. Lancet 388:3017-3026.
9. Mercuri E, BT Darras, CA Chiriboga, JW Day, C Campbell, AM Connolly, ST Iannaccone, J Kirschner, NL Kuntz, et al. (2018). Nusinersen versus Sham Control in Later-Onset Spinal Muscular Atrophy. N Engl J Med 378:625-635.
10. Lim SR and KJ Hertel. (2001). Modulation of survival motor neuron pre-mRNA splicing by inhibition of alternative 3' splice site pairing. J Biol Chem 276:45476-83.

Stem Cells and Development
A *SMN2* splicing modifier rescues the disease phenotypes in an *in vitro* human spinal muscular atrophy model (DOI: 10.1089/scd.2018.0181)
This paper has been peer-reviewed and accepted for publication, but has yet to undergo copyediting and proof correction. The final published version may differ from this proof.

11. Azzouz M, T Le, GS Ralph, L Walmsley, UR Monani, DC Lee, F Wilkes, KA Mitrophanous, SM Kingsman, et al. (2004). Lentivector-mediated SMN replacement in a mouse model of spinal muscular atrophy. J Clin Invest 114:1726-31.

12. Nizzardo M, M Nardini, D Ronchi, S Salani, C Donadoni, F Fortunato, G Colciago, M Falcone, C Simone, et al. (2011). Beta-lactam antibiotic offers neuroprotection in a spinal muscular atrophy model by multiple mechanisms. Exp Neurol 229:214-25.

13. Schmid A and CJ DiDonato. (2007). Animal models of spinal muscular atrophy. J Child Neurol 22:1004-12.

14. Nurputra DK, PS Lai, NI Harahap, S Morikawa, T Yamamoto, N Nishimura, Y Kubo, A Takeuchi, T Saito, et al. (2013). Spinal muscular atrophy: from gene discovery to clinical trials. Ann Hum Genet 77:435-63.

15. Hargus G, M Ehrlich, AL Hallmann and T Kuhlmann. (2014). Human stem cell models of neurodegeneration: a novel approach to study mechanisms of disease development. Acta Neuropathol 127:151-73.

16. Xu XH and Z Zhong. (2013). Disease modeling and drug screening for neurological diseases using human induced pluripotent stem cells. Acta Pharmacol Sin 34:755-64.

17. Chang T, W Zheng, W Tsark, S Bates, H Huang, RJ Lin and JK Yee. (2011). Brief report: phenotypic rescue of induced pluripotent stem cell-derived motoneurons of a spinal muscular atrophy patient. Stem Cells 29:2090-3.

18. Corti S, M Nizzardo, C Simone, M Falcone, M Nardini, D Ronchi, C Donadoni, S Salani, G Riboldi, et al. (2012). Genetic correction of human induced pluripotent stem cells from patients with spinal muscular atrophy. Sci Transl Med 4:165ra162.

19. Ebert AD, J Yu, FF Rose, Jr., VB Mattis, CL Lorson, JA Thomson and CN Svendsen. (2009). Induced pluripotent stem cells from a spinal muscular atrophy patient. Nature 457:277-80.

20. Sareen D, AD Ebert, BM Heins, JV McGivern, L Ornelas and CN Svendsen. (2012). Inhibition of apoptosis blocks human motor neuron cell death in a stem cell model of spinal muscular atrophy. PLoS One 7:e39113.

Stem Cells and Development
A *SMN2* splicing modifier rescues the disease phenotypes in an *in vitro* human spinal muscular atrophy model (DOI: 10.1089/scd.2018.0181)
This paper has been peer-reviewed and accepted for publication, but has yet to undergo copyediting and proof correction. The final published version may differ from this proof.

21. Wang ZB, X Zhang and XJ Li. (2013). Recapitulation of spinal motor neuron-specific disease phenotypes in a human cell model of spinal muscular atrophy. Cell Res 23:378-93.

22. Ohuchi K, M Funato, Z Kato, J Seki, C Kawase, Y Tamai, Y Ono, Y Nagahara, Y Noda, et al. (2016). Established Stem Cell Model of Spinal Muscular Atrophy Is Applicable in the Evaluation of the Efficacy of Thyrotropin-Releasing Hormone Analog. Stem Cells Transl Med 5:152-63.

23. Jung KB, YS Son, H Lee, CR Jung, J Kim and MY Son. (2017). Transcriptome dynamics of human pluripotent stem cell-derived contracting cardiomyocytes using an embryoid body model with fetal bovine serum. Mol Biosyst 13:1565-1574.

24. Son MY, H Sim, YS Son, KB Jung, MO Lee, JH Oh, SK Chung, CR Jung and J Kim. (2017). Distinctive genomic signature of neural and intestinal organoids from familial Parkinson's disease patient-derived induced pluripotent stem cells. Neuropathol Appl Neurobiol 43:584-603.

25. Jung KB, H Lee, YS Son, MO Lee, YD Kim, SJ Oh, O Kwon, S Cho, HS Cho, et al. (2018). Interleukin-2 induces the in vitro maturation of human pluripotent stem cell-derived intestinal organoids. Nat Commun 9:3039.

26. Marquis J, K Meyer, L Angehrn, SS Kampfer, B Rothen-Rutishauser and D Schumperli. (2007). Spinal muscular atrophy: SMN2 pre-mRNA splicing corrected by a U7 snRNA derivative carrying a splicing enhancer sequence. Mol Ther 15:1479-86.

27. Zhang Z, F Lotti, K Dittmar, I Younis, L Wan, M Kasim and G Dreyfuss. (2008). SMN deficiency causes tissue-specific perturbations in the repertoire of snRNAs and widespread defects in splicing. Cell 133:585-600.

28. Chang HC, WC Hung, YJ Chuang and YJ Jong. (2004). Degradation of survival motor neuron (SMN) protein is mediated via the ubiquitin/proteasome pathway. Neurochem Int 45:1107-12.

29. Cho S and G Dreyfuss. (2010). A degron created by SMN2 exon 7 skipping is a principal contributor to spinal muscular atrophy severity. Genes Dev 24:438-42.

30. Jung KB, H Lee, YS Son, JH Lee, HS Cho, MO Lee, JH Oh, J Lee, S Kim, et al. (2018). In vitro and in vivo imaging and tracking of intestinal organoids from human induced pluripotent stem cells. FASEB J 32:111-122.

Stem Cells and Development
A *SMN2* splicing modifier rescues the disease phenotypes in an *in vitro* human spinal muscular atrophy model (DOI: 10.1089/scd.2018.0181)
This paper has been peer-reviewed and accepted for publication, but has yet to undergo copyediting and proof correction. The final published version may differ from this proof.

31. Kim SK, K Kim, JW Ryu, TY Ryu, JH Lim, JH Oh, JK Min, CR Jung, R Hamamoto, et al. (2019). The novel prognostic marker, EHMT2, is involved in cell proliferation via HSPD1 regulation in breast cancer. Int J Oncol 54:65-76.

32. Oh JH, CR Jung, MO Lee, J Kim and MY Son. (2018). Comparative analysis of human embryonic stem cellderived neural stem cells as an in vitro human model. Int J Mol Med 41:783-790.

33. Du ZW, H Chen, H Liu, J Lu, K Qian, CL Huang, X Zhong, F Fan and SC Zhang. (2015). Generation and expansion of highly pure motor neuron progenitors from human pluripotent stem cells. Nat Commun 6:6626.

34. Poudel I, JS Lee, L Tan and JY Lim. (2013). Micropatterning-retinoic acid co-control of neuronal cell morphology and neurite outgrowth. Acta Biomater 9:4592-8.

35. Choi M, J Baek, SB Han and S Cho. (2018). Facile analysis of protein-protein interactions in living cells by enriched visualization of the p-body. BMB Rep 51:526-531.

36. Ning K, C Drepper, CF Valori, M Ahsan, M Wyles, A Higginbottom, T Herrmann, P Shaw, M Azzouz, et al. (2010). PTEN depletion rescues axonal growth defect and improves survival in SMN-deficient motor neurons. Hum Mol Genet 19:3159-68.

37. Monani UR. (2005). Spinal muscular atrophy: a deficiency in a ubiquitous protein; a motor neuron-specific disease. Neuron 48:885-96.

38. Gumireddy K, MV Reddy, SC Cosenza, R Boominathan, SJ Baker, N Papathi, J Jiang, J Holland and EP Reddy. (2005). ON01910, a non-ATP-competitive small molecule inhibitor of Plk1, is a potent anticancer agent. Cancer Cell 7:275-86.

39. Bebee TW, CE Dominguez, S Samadzadeh-Tarighat, KL Akehurst and DS Chandler. (2012). Hypoxia is a modifier of SMN2 splicing and disease severity in a severe SMA mouse model. Hum Mol Genet 21:4301-13.

40. Chen H, K Qian, Z Du, J Cao, A Petersen, H Liu, LWt Blackbourn, CL Huang, A Errigo, et al. (2014). Modeling ALS with iPSCs reveals that mutant SOD1 misregulates neurofilament balance in motor neurons. Cell Stem Cell 14:796-809.

41. Schrank B, R Gotz, JM Gunnersen, JM Ure, KV Toyka, AG Smith and M Sendtner. (1997). Inactivation of the survival motor neuron gene, a candidate gene for human spinal muscular atrophy, leads to massive cell death in early mouse embryos. Proc Natl Acad Sci U S A 94:9920-5.

42. Boza-Moran MG, R Martinez-Hernandez, S Bernal, K Wanisch, E Also-Rallo, A Le Heron, L Alias, C Denis, M Girard, et al. (2015). Decay in survival motor neuron and plastin 3 levels during differentiation of iPSC-derived human motor neurons. Sci Rep 5:11696.

43. Liu H, J Lu, H Chen, Z Du, XJ Li and SC Zhang. (2015). Spinal muscular atrophy patient-derived motor neurons exhibit hyperexcitability. Sci Rep 5:12189.

44. Naryshkin NA, M Weetall, A Dakka, J Narasimhan, X Zhao, Z Feng, KK Ling, GM Karp, H Qi, et al. (2014). Motor neuron disease. SMN2 splicing modifiers improve motor function and longevity in mice with spinal muscular atrophy. Science 345:688-93.

45. Le TT, LT Pham, ME Butchbach, HL Zhang, UR Monani, DD Coovert, TO Gavrilina, L Xing, GJ Bassell, et al. (2005). SMNDelta7, the major product of the centromeric survival motor neuron (SMN2) gene, extends survival in mice with spinal muscular atrophy and associates with full-length SMN. Hum Mol Genet 14:845-57.

46. Mailman MD, JW Heinz, AC Papp, PJ Snyder, MS Sedra, B Wirth, AH Burghes and TW Prior. (2002). Molecular analysis of spinal muscular atrophy and modification of the phenotype by SMN2. Genet Med 4:20-6.

47. Frattini E, M Ruggieri, S Salani, I Faravelli, C Zanetta, M Nizzardo, C Simone, F Magri and S Corti. (2015). Pluripotent stem cell-based models of spinal muscular atrophy. Mol Cell Neurosci 64:44-50.

48. Angelozzi C, F Borgo, FD Tiziano, A Martella, G Neri and C Brahe. (2008). Salbutamol increases SMN mRNA and protein levels in spinal muscular atrophy cells. J Med Genet 45:29-31.

49. Palacino J, SE Swalley, C Song, AK Cheung, L Shu, X Zhang, M Van Hoosear, Y Shin, DN Chin, et al. (2015). SMN2 splice modulators enhance U1-pre-mRNA association and rescue SMA mice. Nat Chem Biol 11:511-7.

50. Hua Y, K Sahashi, F Rigo, G Hung, G Horev, CF Bennett and AR Krainer. (2011). Peripheral SMN restoration is essential for long-term rescue of a severe spinal muscular atrophy mouse model. Nature 478:123-6.

51. Osman EY, MR Miller, KL Robbins, AM Lombardi, AK Atkinson, AJ Brehm and CL Lorson. (2014). Morpholino antisense oligonucleotides targeting intronic repressor Element1 improve phenotype in SMA mouse models. Hum Mol Genet 23:4832-45.

52. Crawford TO, SV Paushkin, DT Kobayashi, SJ Forrest, CL Joyce, RS Finkel, P Kaufmann, KJ Swoboda, D Tiziano, et al. (2012). Evaluation of SMN protein, transcript, and copy number in the biomarkers for spinal muscular atrophy (BforSMA) clinical study. PLoS One 7:e33572.

53. Wirth B, L Brichta, B Schrank, H Lochmuller, S Blick, A Baasner and R Heller. (2006). Mildly affected patients with spinal muscular atrophy are partially protected by an increased SMN2 copy number. Hum Genet 119:422-8.

54. Yoshida M, S Kitaoka, N Egawa, M Yamane, R Ikeda, K Tsukita, N Amano, A Watanabe, M Morimoto, et al. (2015). Modeling the early phenotype at the neuromuscular junction of spinal muscular atrophy using patient-derived iPSCs. Stem Cell Reports 4:561-8.

55. Okabe S, T Tauchi, Y Tanaka, J Sakuta and K Ohyashiki. (2015). Efficacy of the polo-like kinase inhibitor rigosertib, alone or in combination with Abelson tyrosine kinase inhibitors, against break point cluster region-c-Abelson-positive leukemia cells. Oncotarget 6:20231-40.

56. Prasad A, N Khudaynazar, RV Tantravahi, AM Gillum and BS Hoffman. (2016). ON 01910.Na (rigosertib) inhibits PI3K/Akt pathway and activates oxidative stress signals in head and neck cancer cell lines. Oncotarget 7:79388-79400.

57. Komrokji RS, A Raza, JE Lancet, C Ren, D Taft, M Maniar, F Wilhelm and AF List. (2013). Phase I clinical trial of oral rigosertib in patients with myelodysplastic syndromes. Br J Haematol 162:517-24.

58. Hyoda T, T Tsujioka, T Nakahara, S Suemori, S Okamoto, M Kataoka and K Tohyama. (2015). Rigosertib induces cell death of a myelodysplastic syndrome-derived cell line by DNA damage-induced G2/M arrest. Cancer Sci 106:287-93.

Stem Cells and Development
A *SMN2* splicing modifier rescues the disease phenotypes in an *in vitro* human spinal muscular atrophy model (DOI: 10.1089/scd.2018.0181)
This paper has been peer-reviewed and accepted for publication, but has yet to undergo copyediting and proof correction. The final published version may differ from this proof.

59. Bowles DW, JR Diamond, ET Lam, CD Weekes, DP Astling, RT Anderson, S Leong, L Gore, M Varella-Garcia, et al. (2014). Phase I study of oral rigosertib (ON 01910.Na), a dual inhibitor of the PI3K and Plk1 pathways, in adult patients with advanced solid malignancies. Clin Cancer Res 20:1656-65.

60. Ma WW, WA Messersmith, GK Dy, CD Weekes, A Whitworth, C Ren, M Maniar, F Wilhelm, SG Eckhardt, et al. (2012). Phase I study of Rigosertib, an inhibitor of the phosphatidylinositol 3-kinase and Polo-like kinase 1 pathways, combined with gemcitabine in patients with solid tumors and pancreatic cancer. Clin Cancer Res 18:2048-55.

61. Acsadi G, I Lee, X Li, M Khaidakov, A Pecinova, GC Parker and M Huttemann. (2009). Mitochondrial dysfunction in a neural cell model of spinal muscular atrophy. J Neurosci Res 87:2748-56.

62. Berger A, JA Mayr, D Meierhofer, U Fotschl, R Bittner, H Budka, C Grethen, M Huemer, B Kofler, et al. (2003). Severe depletion of mitochondrial DNA in spinal muscular atrophy. Acta Neuropathol 105:245-51.

63. Ripolone M, D Ronchi, R Violano, D Vallejo, G Fagiolari, E Barca, V Lucchini, I Colombo, L Villa, et al. (2015). Impaired Muscle Mitochondrial Biogenesis and Myogenesis in Spinal Muscular Atrophy. JAMA Neurol 72:666-75.

64. Hayashi M, S Araki, N Arai, S Kumada, M Itoh, K Tamagawa, M Oda and Y Morimatsu. (2002). Oxidative stress and disturbed glutamate transport in spinal muscular atrophy. Brain Dev 24:770-5.

Stem Cells and Development
A *SMN2* splicing modifier rescues the disease phenotypes in an *in vitro* human spinal muscular atrophy model (DOI: 10.1089/scd.2018.0181)
This paper has been peer-reviewed and accepted for publication, but has yet to undergo copyediting and proof correction. The final published version may differ from this proof.

Figure legends

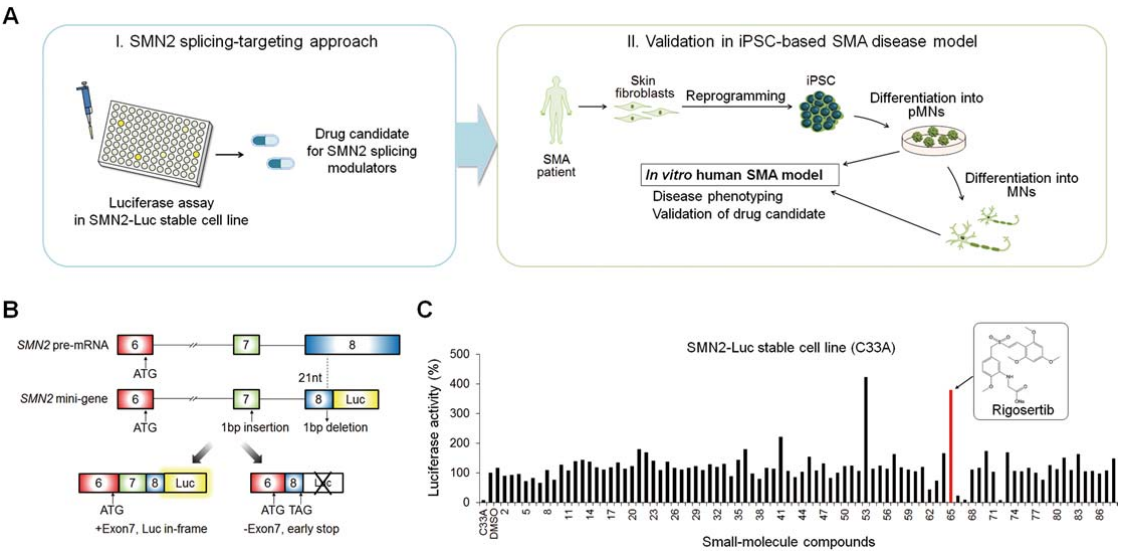

FIG. 1. Exploration of SMN2-specific splicing modulators. **(A)** Schematic diagram of the SMA drug screening platform using the luciferase-based screening system and patient-specific iPSCs. **(B)** Schematic diagram of the *SMN2* minigene reporter and the two protein products generated by alternative splicing. **(C)** Primary screening of small-molecule compounds using SMN2-Luc stable cell lines. SMN2-Luc cells were treated with kinase inhibitors (1 μM) for 24 hours, and luciferase activity was measured. Luciferase activity of No. 65 (rigosertib)-treated cells is shown in the red-coloured column, and the chemical structure of rigosertib is presented in the insert. The percentage of relative luciferase activity was calculated by setting the activity of DMSO-treated cells to 100 %. Naïve C33A cells without the reporter plasmids were included as a negative control. The average and standard deviation were obtained from three independent experiments.

Stem Cells and Development
A *SMN2* splicing modifier rescues the disease phenotypes in an *in vitro* human spinal muscular atrophy model (DOI: 10.1089/scd.2018.0181)
This paper has been peer-reviewed and accepted for publication, but has yet to undergo copyediting and proof correction. The final published version may differ from this proof.

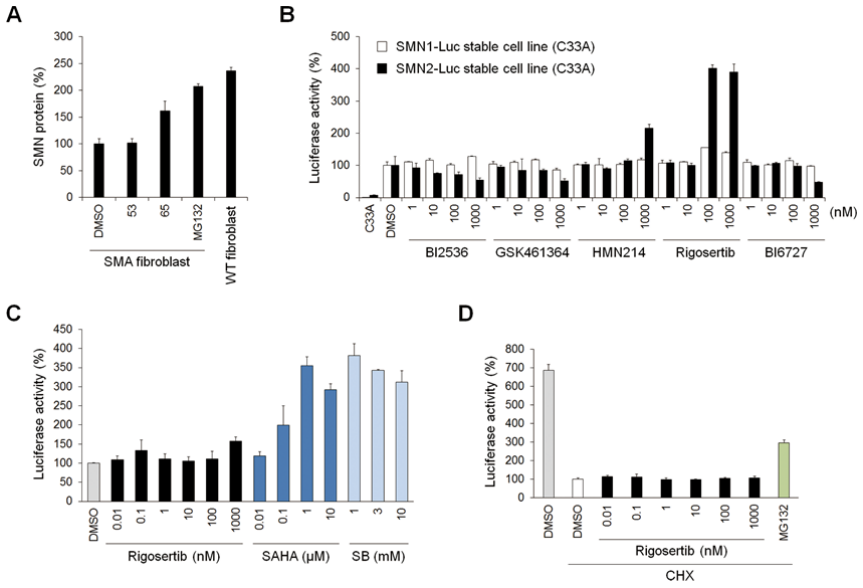

FIG. 2. Compound No. 65, rigosertib, increased SMN protein expression by inducing exon 7 inclusion. **(A)** The amount of SMN protein in SMA patient fibroblasts after treatment with the candidate compounds. SMA fibroblasts were treated with No. 53 and No. 65 (rigosertib) for 24 hours and subjected to an immunoassay, as described in the Materials and Methods. MG132 was used as a positive control, and WT fibroblasts were also included as a cell control. Relative protein amount in percentage was calculated by setting the amount from DMSO-treated cells to 100 %. More than 300 cells for each sample were analysed. **(B)** The effect of five PLK inhibitors on the splicing of SMN2-Luc and SMN1-Luc stable cell lines. Cells were treated with the indicated concentrations for 24 hours, and then luciferase activity was measured. The percentage of relative luciferase activity was calculated by setting the activity of DMSO-treated cells to 100 %. **(C)** Transcriptional activity analysis of compound-induced *SMN2* expression comparing rigosertib, SAHA, and SB. Analysis of the effect of rigosertib on the transcriptional activation of the *SMN2* gene. 293T cells were transfected with pGL4.14-*SMN2* promoter-Luc-PEST plasmids and treated with the indicated concentrations of rigosertib, SAHA and SB. After 24 hours, luciferase activity was measured. **(D)** Analysis of the effect of rigosertib on the protein stability of SMNΔ7. FLuc-SMNΔ7 stable cell lines were treated with the indicated concentrations of rigosertib in the presence of CHX (0.1 mg/ml) for 10 hours, and then luciferase activity was measured. MG132 (10 μM) was included as a positive control. The relative activity was calculated by setting the activity of cells co-treated with DMSO and CHX to 100 %.

Stem Cells and Development
A *SMN2* splicing modifier rescues the disease phenotypes in an *in vitro* human spinal muscular atrophy model (DOI: 10.1089/scd.2018.0181)

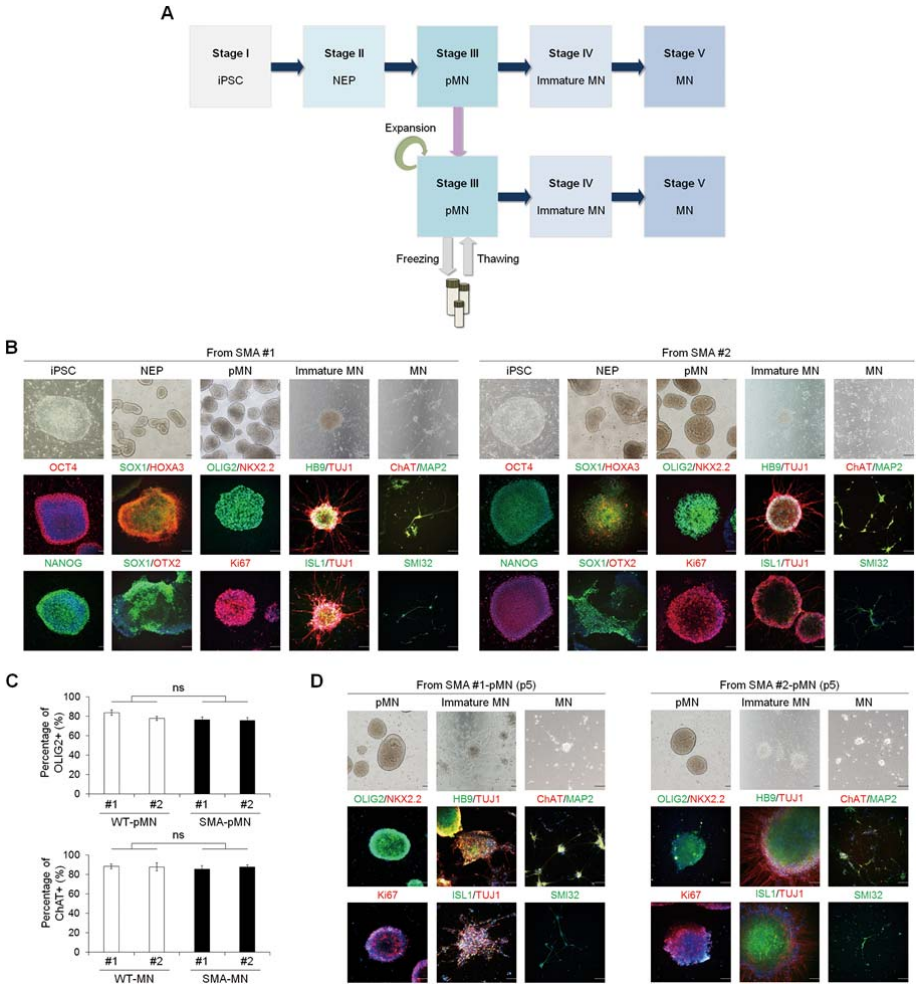

FIG. 3. Differentiation of SMA iPSCs into pMNs and MNs. **(A)** Schematic of the differentiation strategy for MN differentiation. pMNs were induced from iPSCs through the NEP stage and incubated with pMN induction factors for 12 days. pMNs were terminally differentiated into MNs. pMNs can be passaged and expanded for freezing and thawing. **(B)** Immunocytochemistry for lineage-specific markers to identify each cell type during MN differentiation. **(C)** The percentages of OLIG2+ and ChAT+ cells per total DAPI+ cells in the differentiated pMNs and MNs, respectively. (ns; not significant) **(D)** pMNs at passage 5 were also terminally differentiated into MNs. Nuclei were counterstained with DAPI. Scale bar, 100µm.

Stem Cells and Development
A *SMN2* splicing modifier rescues the disease phenotypes in an *in vitro* human spinal muscular atrophy model (DOI: 10.1089/scd.2018.0181)
This paper has been peer-reviewed and accepted for publication, but has yet to undergo copyediting and proof correction. The final published version may differ from this proof.

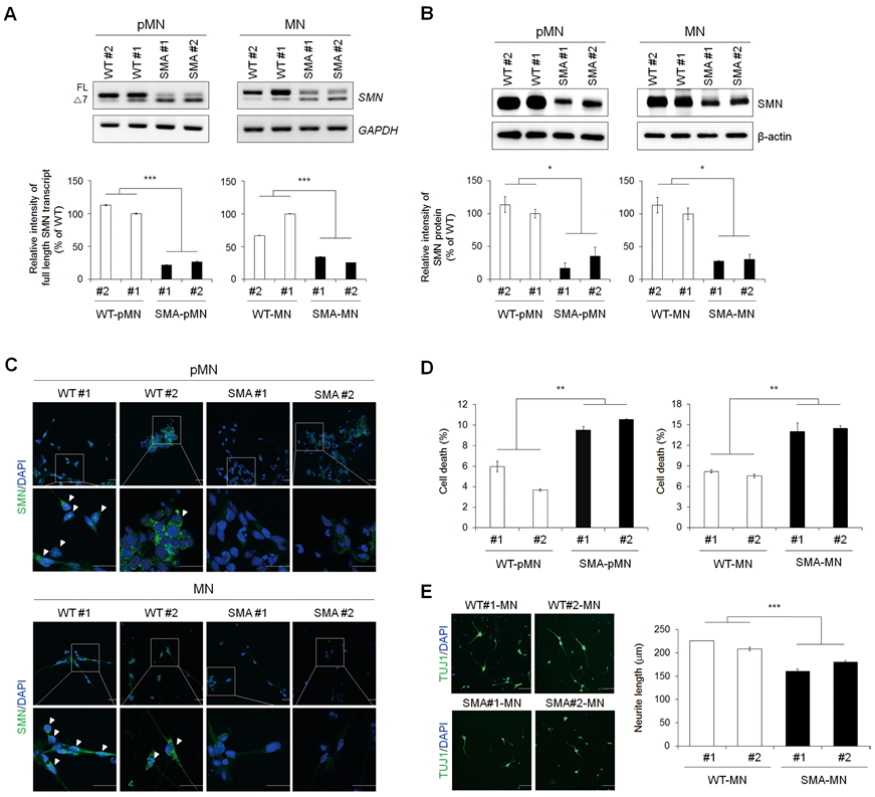

FIG. 4. Phenotypic analysis of WT and SMA iPSC-derived pMNs and MNs. **(A)** RT-PCR analysis for full-length (FL) *SMN* and SMNΔ7 transcript levels in pMNs and MNs. Relative intensity of FL transcript in SMA cells compared with WT control. **(B)** Expression analysis of SMN protein levels by western blotting in pMNs and MNs. Relative intensity of SMN protein in SMA cells compared with WT control. **(C)** Expression analysis of SMN protein levels by immunocytochemistry in pMNs and MNs. Gem bodies (arrowhead) were rarely detected in SMA cells. Scale bar, 20μm. **(D)** Quantitative analysis of the percent of EthD-1+ dead cells in WT and SMA iPSC-derived pMNs and MNs. SMA cells displayed increased EthD-1 signals compared with WT cells (n=3). **(E)** Analysis and quantification of neurite outgrowth. (n=50). Scale bar, 100μm. Data represent the mean ± s.e.m. $^{**}P < 0.01$, $^{*}P < 0.05$, based on Mann-Whitney U-test.

Stem Cells and Development

A *SMN2* splicing modifier rescues the disease phenotypes in an *in vitro* human spinal muscular atrophy model (DOI: 10.1089/scd.2018.0181)

This paper has been peer-reviewed and accepted for publication, but has yet to undergo copyediting and proof correction. The final published version may differ from this proof.

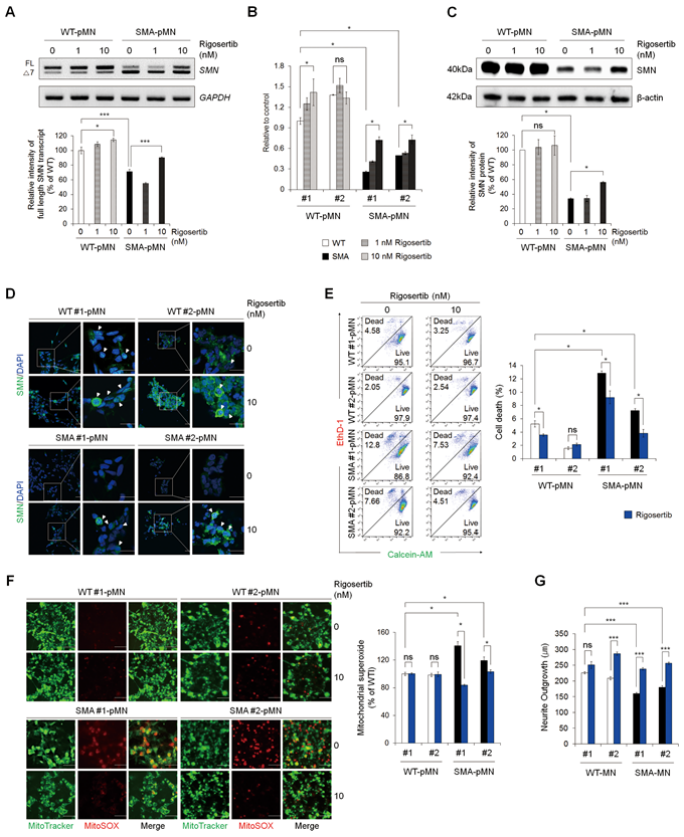

FIG. 5. Restoration of *SMN2* exon 7 splicing rescued SMA-like phenotypes in SMA iPSC-pMNs by rigosertib treatment. **(A)** RT-PCR analysis confirmed a pronounced shift of *SMN2* transcripts from SMNΔ7 to SMN-FL. The gel and western blot images are representative of three separate experiments. Data are the means ± s.e.m of three independent experiments. **(B)** Quantitative analysis of SMN-FL expression using qRT-PCR (n=3). The expression of SMN-FL was increased by treatment with rigosertib in SMA iPSC-derived pMNs. Expression analysis of SMN protein levels by western blotting **(C)** and immunocytochemistry **(D)** in pMNs after 10 nM rigosertib treatment for 72 hr. Rigosertib treatment restored gem body formation in SMA iPSC-pMNs (arrowhead). Scale bar, 20μm. **(E)** Flow cytometry viability assay showing live cells stained with Calcein-AM (green) and dead cells stained with EthD-1 (red). The ratio of dead cells was decreased in 10 nM rigosertib-treated SMA iPSC-pMNs (n≥3). **(F)** WT and SMA iPSC-derived pMNs labelled with MitoTracker Green and MitoSOX. Superoxide levels expressed as a MitoSOX/MitoTracker ratio (superoxide signal/total mitochondrial signal). Mitochondrial superoxide overproduction (MitoSOX, red) in SMA iPSC-pMNs was attenuated by 10 nM rigosertib

treatment (n=3). Scale bar, 100 μm. Data represent the mean ± s.e.m. **P* < 0.05, based on Mann-Whitney U-test. **(G)** The effect of rigosertib on neurite length in iPSC-derived MNs. Quantification of neurite outgrowth in WT iPSC-MNs and SMA iPSC-MNs in the presence or absence of 1 nM rigosertib (n=50 for each condition). Data represent the mean ± s.e.m. ****P* < 0.001 based on Mann-Whitney U-test.

Stem Cells and Development
A *SMN2* splicing modifier rescues the disease phenotypes in an *in vitro* human spinal muscular atrophy model (DOI: 10.1089/scd.2018.0181)
This paper has been peer-reviewed and accepted for publication, but has yet to undergo copyediting and proof correction. The final published version may differ from this proof.

Stem Cells and Development
A *SMN2* splicing modifier rescues the disease phenotypes in an *in vitro* human spinal muscular atrophy model (DOI: 10.1089/scd.2018.0181)
This paper has been peer-reviewed and accepted for publication, but has yet to undergo copyediting and proof correction. The final published version may differ from this proof.

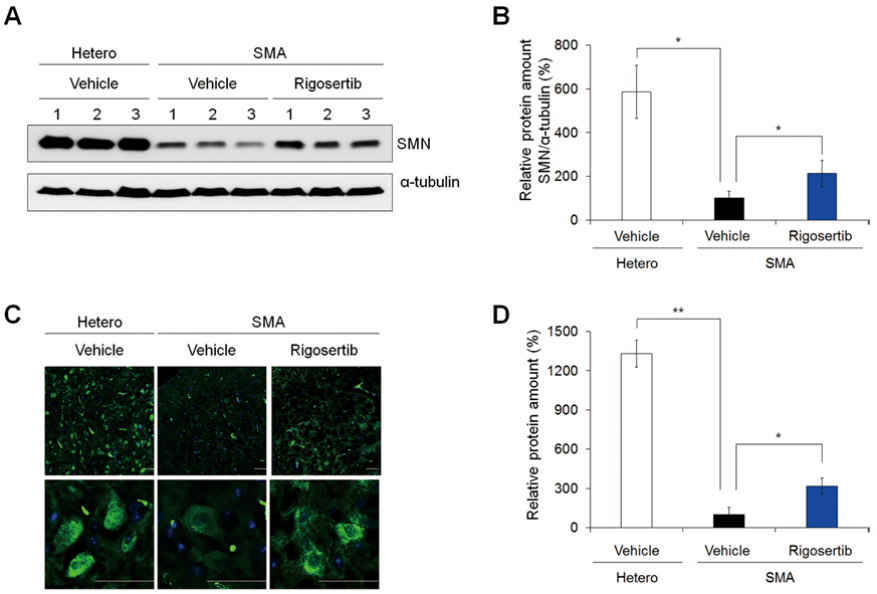

FIG. 6. Rigosertib increases the amount of SMN protein in the spinal cord of SMA mice. **(A)** Spinal cords were isolated from heterozygous, vehicle-treated, and rigosertib (10 mg/kg)-treated SMA mice (n=3 for each) and analyzed by western blotting with anti-SMN antibody. α-Tubulin was also analyzed as a loading control. **(B)** Protein bands were quantified and the band intensities for vehicle-treated SMA were set as 100 %. **(C)** Expression of SMN protein levels by immunohistochemistry in spinal cord sections and **(D)** relative cell counts of SMN-positive cells compared to the heterozygous group (n=3). Scale bar, 50 µm. Data represent the mean ± s.e.m. $^{**}P < 0.01$, $^{*}P < 0.05$, based on Mann-Whitney U-test. The green background staining represents blood capillaries.

Supplementary Table S1. PCR primer sequences used in this study.

Target gene	RT-Forward	RT-Reverse
OCT4	GAGGAGTCCCAGGACATCAA	AATAGAACCCCCAGGGTGAG
NANOG	CAAAGGCAAACAACCCACTT	ATTGTTCCAGGTCTGGTTGC
GAPDH	GAA GGT GAA GGT CGG AGT C	GAA GAT GGT GAT GGG ATT TC
SMN2	GGAAAGCCAGGTCTAAAATTCAA	CTATAACGCTTCACATTCCAGAT
SMN exon 7-8	GCTCACATTCCTTAAATTAAGGAGAAA	TCCAGATCTGTCTGATCGTTTCTT

Stem Cells and Development
A *SMN2* splicing modifier rescues the disease phenotypes in an *in vitro* human spinal muscular atrophy model (DOI: 10.1089/scd.2018.0181)
This paper has been peer-reviewed and accepted for publication, but has yet to undergo copyediting and proof correction. The final published version may differ from this proof.

Supplementary Table S2. Information of the antibodies used in this study.

Antibodies	Catalog No.	Company	Dilution
Pluripotency markers			
anti-OCT4	sc-9081	Santa Cruz	1:100 for IF
anti-NANOG	AF1997	R&D	1:40 for IF
anti-SSEA-3	MAB4303	Millipore	1:30 for IF
anti-SSEA-4	MAB4304	Millipore	1:30 for IF
anti-TRA-1-60	MAB4360	Millipore	1:100 for IF
anti-TRA-1-81	MAB4381	Millipore	1:100 for IF
Three germ layer markers			
anti-TUJ1	PRB-435P	Covance	1:500 for IF
anti-NESTIN	MAB5326	Millipore	1:100 for IF
anti-FOXA2	07-633	Millipore	1:100 for IF
anti-SOX17	MAB1924	R&D	1:50 for IF
anti-α-SMA	A5228	Sigma	1:200 for IF
anti-DESMIN	AB907	Chemicon	1:50 for IF
Motor neuron differentiation markers			
anti-SOX1	AF3369	R&D	1:100 for IF
anti-SOX1	AB15766	Millipore	1:100 for IF
anti-OTX2	AF1979	R&D	1:100 for IF
anti-HOXA3	HPA029157	Sigma-aldrich	1:100 for IF
anti-OLIG2	AB9610	Chemicon	1:100 for IF
anti-NKX2.2	74.5A5	DSHB	1:100 for IF
anti-Ki67	AB9260	Chemicon	1:100 for IF
anti-MNX1	81.5C10	DSHB	1:100 for IF
anti-ISL1	40.2D6	DSHB	1:100 for IF

Stem Cells and Development
A *SMN2* splicing modifier rescues the disease phenotypes in an *in vitro* human spinal muscular atrophy model (DOI: 10.1089/scd.2018.0181)
This paper has been peer-reviewed and accepted for publication, but has yet to undergo copyediting and proof correction. The final published version may differ from this proof.

anti-TUJ1	PRB-435P	Covance	1:100 for IF
anti-ChAT	AB144P	Chemicon	1:100 for IF
anti-MAP2	MAB3418	Chemicon	1:100 for IF
Anti-Neurofilament heavy polypeptide antibody	Ab7795	Abcam	1:500 for IF
SMN protein			
anti-SMN	610647	BD	1:5000 for WB 1:100 for IF 1:300 for IHC
Anti- β-actin	sc-81178	Santa Cruz	1:2000 for WB
Neuromuscular junction			
α-Bungarotoxin-488	B13422	Molecular probes	1:100 for IF

*IF: Immunofluorescence

*WB: Western blotting

*IHC: Immunohistochemistry

Stem Cells and Development
A *SMN2* splicing modifier rescues the disease phenotypes in an *in vitro* human spinal muscular atrophy model (DOI: 10.1089/scd.2018.0181)
This paper has been peer-reviewed and accepted for publication, but has yet to undergo copyediting and proof correction. The final published version may differ from this proof.

Supplementary Table S3. List of screened compounds used in this study.

No.	Compound	No.	Compound
1	DMSO	2	BMS-599626
3	Erlotinib Hydrochloride	4	Gefitinib(Iressa)
5	Neratinib	6	PD153035 hydrochloride
7	Pelitinib	8	Vandetanib
9	WZ3146	10	WZ4002
11	WZ8040	12	AV-951(Tivozanib)
13	Axitinib	14	BIBF1120(Vargatef)
15	BMS 794833	16	DMSO
17	Cediranib(AZD2171)	18	DMSO
19	CYC116	20	DMSO
21	Imatinib(STI571)	22	Imatinib Mesylate
23	Ki8751	24	KRN 633
25	Masitinib(AB1010)	26	MGCD-265
27	Motesanib Diphosphate	28	Amuvatinib
29	OSI-930	30	Pazopanib Hydrochloride
31	Sorafenib Tosylate	32	Sunitinib Malate
33	TSU-68	34	Vatalanib
35	XL880(GSK1363089)	36	PHA-739358(Danusertib)
37	AT9283	38	AZD0530(Saracatinib)
39	Bosutinib(SKI-606)	40	Dasatinib
41	Nilotinib	42	Quercetin(Sophoretin)
43	NVP-ADW742	44	Quizartinib
45	AP24534	46	Tandutinib (MLN518)
47	KW 2449	48	CI-1033(Canertinib)
49	CP-724714	50	BAY 73-4506(Regorafenib)
51	JNJ-38877605	52	PF-04217903
53	Crizotinib (PF-02341066)	54	DMSO

Stem Cells and Development
A *SMN2* splicing modifier rescues the disease phenotypes in an *in vitro* human spinal muscular atrophy model (DOI: 10.1089/scd.2018.0181)
This paper has been peer-reviewed and accepted for publication, but has yet to undergo copyediting and proof correction. The final published version may differ from this proof.

55	SGX-523	56	SU11274(PKI-SU11274)
57	NVP-TAE684	58	SB 525334
59	R406	60	R406(free base)
61	XL184	62	BI 2536
63	GSK461364	64	HMN-214
65	ON-01910 (Rigosertib)	66	AT7519
67	Flavopiridol(Alvocidib)	68	BS-181 hydrochloride
69	PD0332991	70	PHA-793887
71	Roscovitine(CYC202)	72	SNS-032(BMS-387032)
73	AZD7762	74	Aurora A Inhibitor I
75	Barasertib	76	CCT129202
77	ENMD-2076	78	Hesperadin
79	MLN8237	80	DMSO
81	PHA-680632	82	SNS-314 Mesylate
83	VX-680	84	ZM-447439
85	AS703026	86	AZD6244(Selumetinib)
87	AZD8330	88	BIX 02188

Stem Cells and Development
A *SMN2* splicing modifier rescues the disease phenotypes in an *in vitro* human spinal muscular atrophy model (DOI: 10.1089/scd.2018.0181)
This paper has been peer-reviewed and accepted for publication, but has yet to undergo copyediting and proof correction. The final published version may differ from this proof.

Supplementary Figure legends

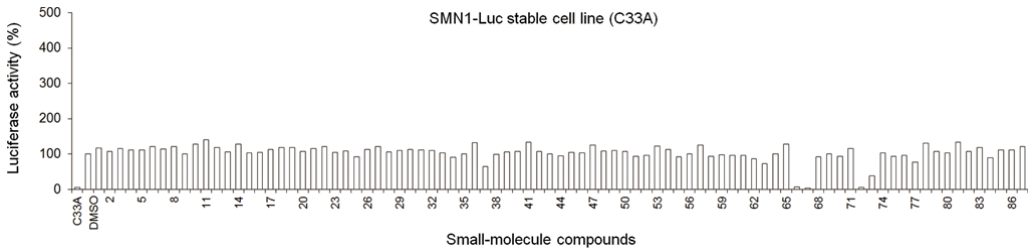

Supplementary FIG. S1. Effect of small-molecule treatments in the SMN1-Luc stable cell line. SMN1-Luc cells were treated with kinase inhibitors (1 μM) for 24 hours, and luciferase activity was measured. The percentage of relative luciferase activity was calculated by setting the activity from DMSO-treated cells to 100 %. The average and standard deviation were obtained from three independent experiments.

Stem Cells and Development
A *SMN2* splicing modifier rescues the disease phenotypes in an *in vitro* human spinal muscular atrophy model (DOI: 10.1089/scd.2018.0181)
This paper has been peer-reviewed and accepted for publication, but has yet to undergo copyediting and proof correction. The final published version may differ from this proof.

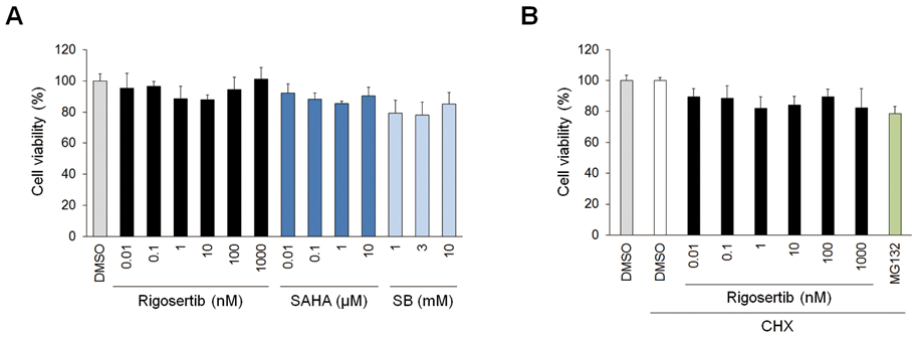

Supplementary FIG. S2. The effect of small molecule treatment on cell viability in the *SMN2* reporter system for *SMN2* promoter activity **(A)** and SMNΔ7 protein stability **(B)**. Cell viability was measured using CellTiter-Glo reagent. The relative activity was calculated by setting the activity of DMSO-treated cells to 100 %.

Stem Cells and Development
A *SMN2* splicing modifier rescues the disease phenotypes in an *in vitro* human spinal muscular atrophy model (DOI: 10.1089/scd.2018.0181)
This paper has been peer-reviewed and accepted for publication, but has yet to undergo copyediting and proof correction. The final published version may differ from this proof.

Stem Cells and Development
A *SMN2* splicing modifier rescues the disease phenotypes in an *in vitro* human spinal muscular atrophy model (DOI: 10.1089/scd.2018.0181)
This paper has been peer-reviewed and accepted for publication, but has yet to undergo copyediting and proof correction. The final published version may differ from this proof.

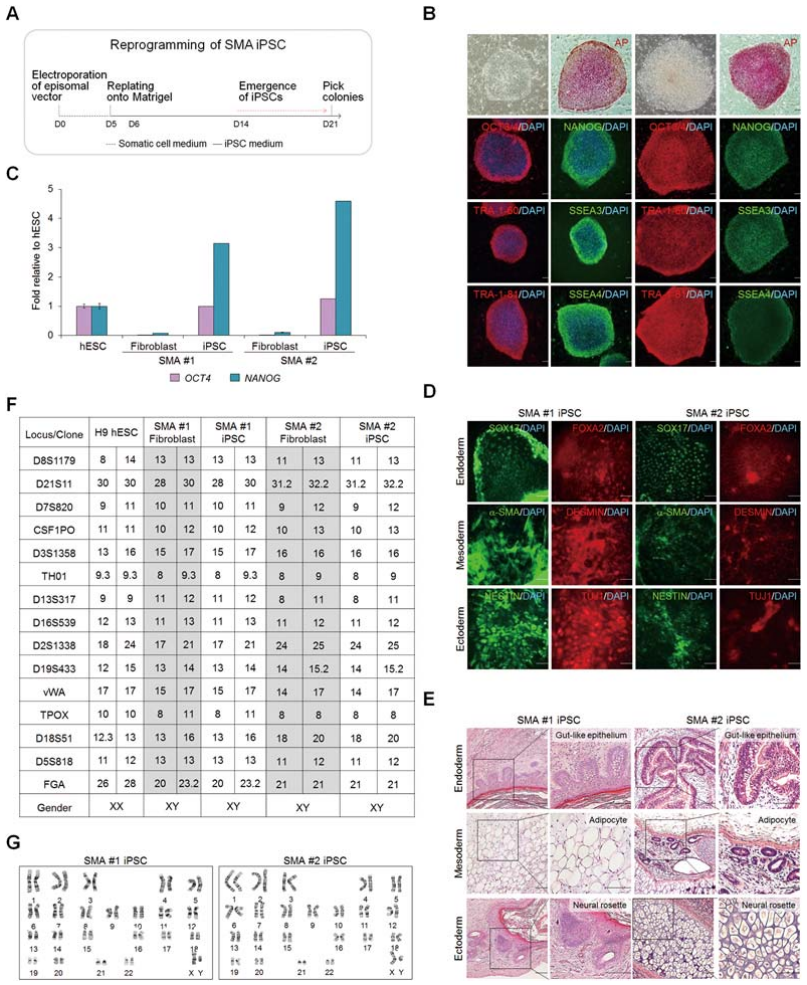

Locus/Clone	H9 hESC		SMA #1 Fibroblast		SMA #1 iPSC		SMA #2 Fibroblast		SMA #2 iPSC	
D8S1179	8	14	13	13	13	13	11	13	11	13
D21S11	30	30	28	30	28	30	31.2	32.2	31.2	32.2
D7S820	9	11	10	11	10	11	9	12	9	12
CSF1PO	11	11	10	12	10	12	10	13	10	13
D3S1358	13	16	15	17	15	17	16	16	16	16
TH01	9.3	9.3	8	9.3	8	9.3	8	9	8	9
D13S317	9	9	11	12	11	12	8	11	8	11
D16S539	12	13	11	13	11	13	11	12	11	12
D2S1338	18	24	17	21	17	21	24	25	24	25
D19S433	12	15	13	14	13	14	14	15.2	14	15.2
vWA	17	17	15	17	15	17	14	17	14	17
TPOX	10	10	8	11	8	11	8	8	8	8
D18S51	12.3	13	13	16	13	16	18	20	18	20
D5S818	11	12	13	13	13	13	11	12	11	12
FGA	26	28	20	23.2	20	23.2	21	21	21	21
Gender	XX		XY		XY		XY		XY	

Supplementary FIG. S3. Generation and characterization of SMA-specific iPSCs. **(A)** Schematic of the reprogramming process for SMA patient-derived iPSCs. **(B)** AP staining and immunocytochemistry of SMA iPSCs for pluripotency markers including OCT4, TRA-1-60, TRA-1-81, NANOG, SSEA-3, and SSEA-4. Scale bar, 100 µm. **(C)** qRT-PCR analysis for *OCT4* and *NANOG*. **(D)** *In vitro* differentiation of SMA-specific iPSCs *via* EB formation. Immunocytochemistry for markers of the three germ layers using antibodies for ectoderm (NESTIN and TUJ1), mesoderm (α-SMA and DESMIN), and endoderm (SOX17 and FOXA2) markers. Scale bar, 100µm. **(E)** *In vivo* differentiation of SMA-specific iPSCs for teratoma formation. Haematoxylin and eosin-stained sections from teratomas generated from SMA-specific iPSCs. **(F)** STR analysis with SMA patient fibroblasts and SMA iPSCs. **(G)** Karyotype analysis using SMA iPSCs.

Stem Cells and Development
A *SMN2* splicing modifier rescues the disease phenotypes in an *in vitro* human spinal muscular atrophy model (DOI: 10.1089/scd.2018.0181)
This paper has been peer-reviewed and accepted for publication, but has yet to undergo copyediting and proof correction. The final published version may differ from this proof.

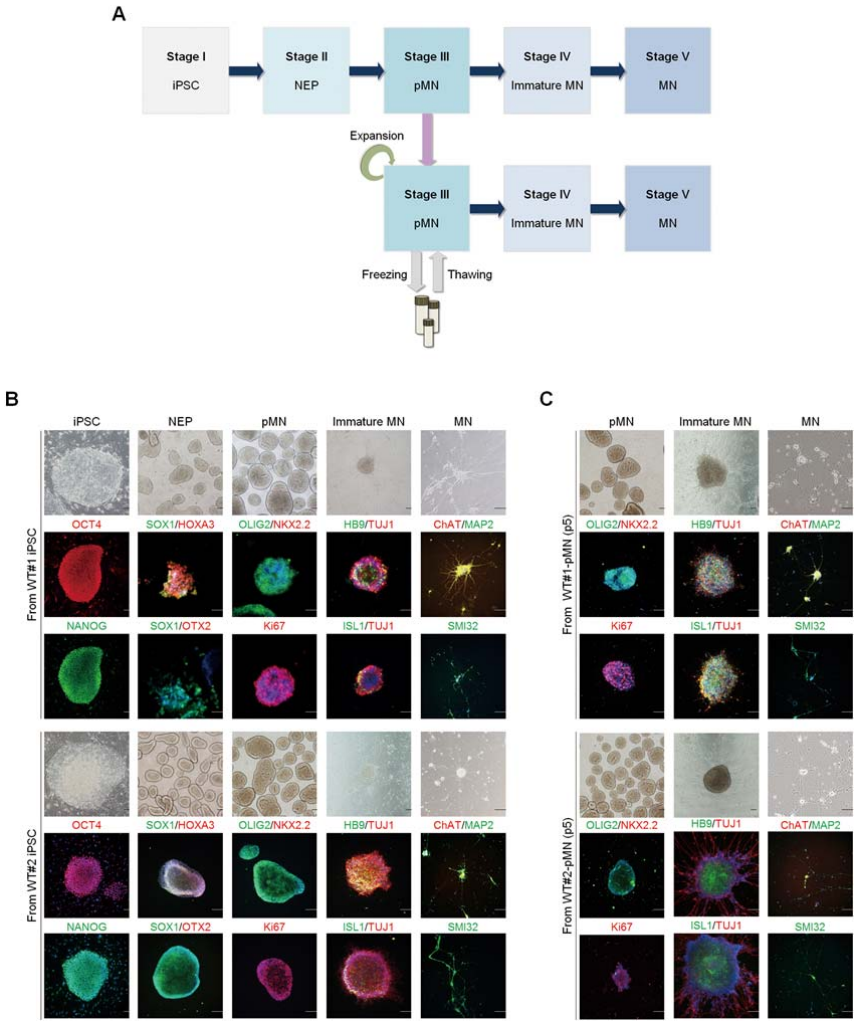

Supplementary FIG. S4. Differentiation towards pMNs and MNs from WT iPSCs. **(A)** Schematic of the differentiation strategy for MN differentiation. pMNs were induced from iPSCs through the NEP stage and incubated with pMN induction factors for 12 days. pMNs were terminally differentiated into MNs. pMNs can be passaged and expanded for freezing and thawing. **(B)** Immunocytochemistry of lineage-specific markers to identify each cell type during MN differentiation. **(C)** pMNs at passage 5 were also terminally differentiated into MNs. Nuclei were counterstained with DAPI. Scale bar, 100µm.

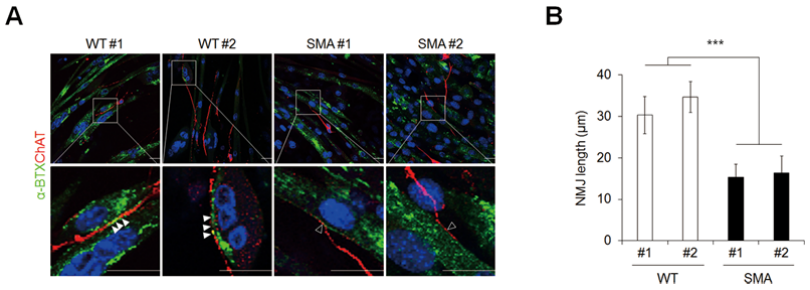

Supplementary FIG. S5. Neuromuscular junction formation assay. MNs, stained with the ChAT antibody (red), formed neuromuscular junctions, labelled with α-bungarotoxin (α-BTX, green), when co-cultured with myotubes of differentiated C2C12 cells. **(A)** Representative images for neuromuscular junction in co-cultured with WT and SMA iPSC-MNs and C2C12 cell lines. Scale bar, 20 μm. **(B)** Quantification of neuromuscular junction. Data represent the mean ± s.e.m. ***$P < 0.001$ based on Mann-Whitney U-test.

Stem Cells and Development
A *SMN2* splicing modifier rescues the disease phenotypes in an *in vitro* human spinal muscular atrophy model (DOI: 10.1089/scd.2018.0181)
This paper has been peer-reviewed and accepted for publication, but has yet to undergo copyediting and proof correction. The final published version may differ from this proof.

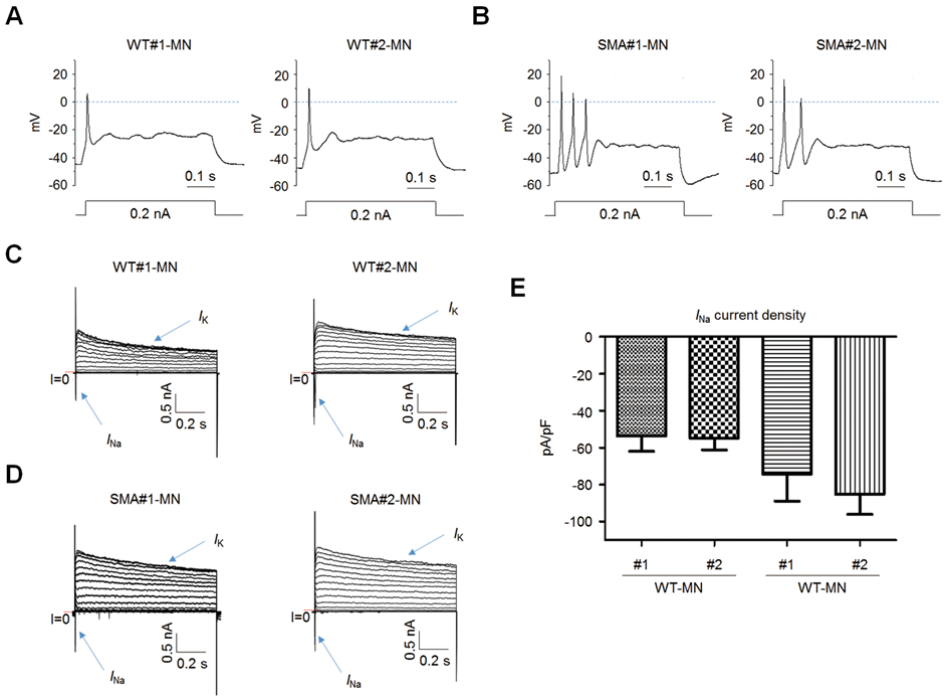

Supplementary FIG. S6. Functional analysis of terminally differentiated MNs derived from WT and SMA iPSCs. (A) Representative traces of membrane potential changes induced by current injection step of 0.2 nA for 500 ms in WT iPSC-MNs. (B) Representative membrane voltage traces upon stem injection of current in SMA iPSC-MNs. (C) Representative whole-cell currents for recording of voltage-gated inward Na^+ (I_{Na}) and outward K^+ (I_K) currents induced by depolarizing voltage steps (from −70 to +90 mV for 1 s in 10 mV increments) on WT iPSC-MNs. (D) Representative I_{Na} and I_K currents induced by depolarizing voltage steps on SMA iPSC-MNs. (E) Summary of the I_{Na} current density at -10 mV for each group (n = 6 in WT#1 iPSC-MNs, each n = 4 in the other groups).

Stem Cells and Development
A *SMN2* splicing modifier rescues the disease phenotypes in an *in vitro* human spinal muscular atrophy model (DOI: 10.1089/scd.2018.0181)
This paper has been peer-reviewed and accepted for publication, but has yet to undergo copyediting and proof correction. The final published version may differ from this proof.